Documentation for VP:
Nonlinear Vlasov-Poisson Simulation Code

2016

Contents

Chapter 1

Theory for Landau Damping in a 1D1V Vlasov-Poisson Plasma

The main goal of these analytical calculations is to identify the energy transferred from the electrostatic field to the particles via resonant collisionless wave-particle interactions, and to determine the impact of this resonantly transferred energy on the particle distribution functions. This theoretical insight will be used to devise novel analysis strategies to definitively identify the action of collisionless wave-particle interactions in heliospheric plasmas using spacecraft measurements or nonlinear kinetic numerical simulations.

Note, of course, that the Lorentz term in the Vlasov equation, in addition to governing resonant energy transfer in collisionless wave-particle interactions, also is responsible for the typical oscillatory transfer of energy between fields and particles characteristic of (linear) wave motion. Thus, the problem is to isolate the physics describing the resonant energy transfer from the common linear wave response.

1.1 Vlasov-Poisson Problem

The 1D-1V Vlasov-Poisson system is governed by the Boltzmann equation for the species distribution functions $f_s(x, v, t)$

$$\frac{\partial f_s}{\partial t} + v\frac{\partial f_s}{\partial x} - \frac{q_s}{m_s}\frac{\partial \phi}{\partial x}\frac{\partial f_s}{\partial v} = 0 \tag{1.1}$$

and the Poisson equation for the scalar electrostatic potential $\phi(x, t)$

$$\frac{\partial^2 \phi}{\partial x^2} = -4\pi \sum_s \int_{-\infty}^{+\infty} dv \quad q_s f_s \tag{1.2}$$

1.2 Derivation of Poynting's Theorem and Electrostatic Limit

Poynting's theorem is derived directly from Maxwell's equations, specifically Faraday's Law

$$\frac{\partial \mathbf{B}}{\partial t} = -c\nabla \times \mathbf{E} \tag{1.3}$$

and the Ampere-Maxwell Law,

$$\frac{\partial \mathbf{E}}{\partial t} = c\nabla \times \mathbf{B} - 4\pi \mathbf{j}. \tag{1.4}$$

First, take the dot product of $\mathbf{B}$ with Faraday's Law and the dot product of $\mathbf{E}$ with the Ampere-Maxwell Law and sum the results divided by 4π, to obtain

$$\frac{1}{4\pi}\left(\mathbf{E}\cdot\frac{\partial \mathbf{E}}{\partial t} + \mathbf{B}\cdot\frac{\partial \mathbf{B}}{\partial t}\right) = \frac{1}{4\pi}\left(c\mathbf{E}\cdot\nabla\times\mathbf{B} - c\mathbf{B}\cdot\nabla\times\mathbf{E} - 4\pi\mathbf{j}\cdot\mathbf{E}\right). \tag{1.5}$$

Using the vector identity

$$\nabla\cdot(\mathbf{E}\times\mathbf{B}) = \mathbf{B}\cdot\nabla\times\mathbf{E} - \mathbf{E}\cdot\nabla\times\mathbf{B} \tag{1.6}$$

and

$$\mathbf{E}\cdot\frac{\partial \mathbf{E}}{\partial t} = \frac{1}{2}\frac{\partial |\mathbf{E}|^2}{\partial t}, \tag{1.7}$$

we obtain the form

$$\frac{\partial}{\partial t}\left(\frac{|\mathbf{E}|^2 + |\mathbf{B}|^2}{8\pi}\right) + \frac{c}{4\pi}\nabla\cdot(\mathbf{E}\times\mathbf{B}) = -\mathbf{j}\cdot\mathbf{E} \tag{1.8}$$

Next, we integrate over the volume of the plasma and use Gauss's Theorem to replace the second term by

$$\int d^3\mathbf{x}\ \ \nabla\cdot(\mathbf{E}\times\mathbf{B}) = \oint d^2\mathbf{S}\cdot(\mathbf{E}\times\mathbf{B}), \tag{1.9}$$

thereby obtaining the final result, *Poynting's Theorem*,

$$\frac{\partial}{\partial t}\int d^3\mathbf{x}\frac{|\mathbf{E}|^2 + |\mathbf{B}|^2}{8\pi} + \frac{c}{4\pi}\oint d^2\mathbf{S}\cdot(\mathbf{E}\times\mathbf{B}) = -\int d^3\mathbf{x}\ \ \mathbf{j}\cdot\mathbf{E} \tag{1.10}$$

In the electrostatic limit $\mathbf{B} = 0$, Poynting's Theorem has the form

$$\frac{\partial}{\partial t}\int d^3\mathbf{x}\frac{|\mathbf{E}|^2}{8\pi} = -\int d^3\mathbf{x}\ \ \mathbf{j}\cdot\mathbf{E} \tag{1.11}$$

A shorter derivation of Poynting's Theorem in the electrostatic limit, in this case one dimensional with $\mathbf{k} = k\hat{\mathbf{x}}$ and $\mathbf{E} = E\hat{\mathbf{x}}$, uses the Ampere-Maxwell Law. In this 1D electrostatic limit, the curl term of the Ampere-Maxwell Law is zero, leaving

$$\frac{\partial \mathbf{E}}{\partial t} = -4\pi\mathbf{j}. \tag{1.12}$$

Taking the dot product with respect to $\mathbf{E}$ yields

$$\frac{\partial}{\partial t}\left(\frac{|\mathbf{E}|^2}{8\pi}\right) = -\mathbf{j}\cdot\mathbf{E} \tag{1.13}$$

Note that this strictly electrostatic version does not require the spatial integration (physcially because electrostatic waves have no energy flux and carry no momentum), so this equation is true at each point in space.

1.3 Conservation of Energy in the 1D1V Vlasov-Poisson System

Begin with the Vlasov equation for species s, multiply by $m_s v^2/2$, and integrate over all space (1D) and all velocity (1V) to obtain

$$\int dx \int dv \left(\frac{m_s v^2}{2}\right) \frac{\partial f_s}{\partial t} + \int dx \int dv \left(\frac{m_s v^2}{2}\right) v \frac{\partial f_s}{\partial x} - \int dx \int dv \left(\frac{m_s v^2}{2}\right) \frac{q_s}{m_s} \frac{\partial \phi}{\partial x} \frac{\partial f_s}{\partial v} = 0 \tag{1.14}$$

Using the fact that x, v, and t are independent variables, we can interchange the order of differentiaton and integration and make other simplifications to yield

$$\frac{\partial}{\partial t} \int dx \int dv \frac{1}{2} m_s v^2 f_s + \int dx \frac{\partial}{\partial x} \left[\int dv \frac{1}{2} m_s v^3 f_s \right] - \int dx \frac{\partial \phi}{\partial x} \int dv \left(\frac{q_s v^2}{2}\right) \frac{\partial f_s}{\partial v} = 0 \tag{1.15}$$

The second term is a perfect differential in x, so for either periodic boundary conditions, $f_s(x = -L, v) = f_s(x = L, v)$, or boundaries at infinity, $\lim_{L\to\infty} f_s(x = \pm L, v) = 0$, this term integrates to zero

$$\int dx \frac{\partial}{\partial x} \left[\int dv \frac{1}{2} m_s v^3 f_s \right] = \int dv \frac{1}{2} m_s v^3 f_s(x = L, v) - \int dv \frac{1}{2} m_s v^3 f_s(x = -L, v) = 0 \tag{1.16}$$

In the third term, we can use integration by parts in the velocity integral to convert

$$\int dv \left(\frac{q_s v^2}{2}\right) \frac{\partial f_s}{\partial v} = \left[\frac{q_s v^2}{2} f_s \right]_{-\infty}^{\infty} - \int dv \;\; q_s v f_s \equiv -j_s. \tag{1.17}$$

where the term in brackets is zero since $\lim_{v\to\pm\infty} f_s(x, v) = 0$.

Thus, we obtain the result

$$\frac{\partial}{\partial t} \int dx \int dv \frac{1}{2} m_s v^2 f_s = - \int dx \frac{\partial \phi}{\partial x} j_s = \int dx \;\; j_s E \tag{1.18}$$

where we have used the relation for the electric field in terms of the scalar potential, $E = -\frac{\partial \phi}{\partial x}$. Summing over species to get the total current $j = \sum_s j_s$, we have the relation,

$$\int dx \;\; jE = \sum_s \frac{\partial}{\partial t} \int dx \int dv \frac{1}{2} m_s v^2 f_s \tag{1.19}$$

Using this relation we substitute for the right-hand side of the electrostatic limit of Poynting's Theorem (1.11) to obtain,

$$\frac{\partial}{\partial t} \int d^3\mathbf{x} \frac{|\mathbf{E}|^2}{8\pi} = - \sum_s \frac{\partial}{\partial t} \int d^3\mathbf{x} \int dv \frac{1}{2} m_s v^2 f_s \tag{1.20}$$

A final rearrangement, pulling out the time derivative, leads to the ultimate result for the conservation of energy in the Vlasov-Poisson system,

$$\frac{\partial W}{\partial t} = 0 \tag{1.21}$$

where the *conserved Vlasov-Poisson energy* is given by

$$W = \int d^3\mathbf{x} \frac{|\mathbf{E}|^2}{8\pi} + \sum_s \int d^3\mathbf{x} \int dv \frac{1}{2} m_s v^2 f_s \tag{1.22}$$

For later reference, let us define the separate components of the conserved energy as the *electrostatic field energy*

$$W_\phi \equiv \int d^3\mathbf{x} \frac{|\mathbf{E}|^2}{8\pi}, \tag{1.23}$$

the *microscopic ion kinetic energy*

$$W_i \equiv \int d^3\mathbf{x} \int dv \frac{1}{2} m_i v^2 f_i, \tag{1.24}$$

and the *microscopic electron kinetic energy*

$$W_e \equiv \int d^3\mathbf{x} \int dv \frac{1}{2} m_e v^2 f_e, \tag{1.25}$$

such that the *total conserved Vlasov-Poisson energy* is given by

$$W = W_\phi + W_i + W_e. \tag{1.26}$$

1.4 Transfer of Energy in Collisionless Wave-Particle Interactions

The main goal of these analytical calculations is to identify the energy transferred from the electrostatic field to the particles via resonant collisionless wave-particle interactions, and to determine the impact of this resonantly transferred energy on the particle distribution functions. This theoretical insight will be used to devise novel analysis strategies to definitively identify the action of collisionless wave-particle interactions in heliospheric plasmas using spacecraft measurements or the results of nonlinear kinetic numerical simulations.

First, in the Vlasov-Poisson system, note that the energy gain by the particles must be equal to the energy lost from the electrostatic field,

$$\frac{\partial}{\partial t} \sum_s \int d^3\mathbf{x} \int dv \frac{1}{2} m_s v^2 f_s = -\frac{\partial W_\phi}{\partial t} \tag{1.27}$$

Therefore, the rate of energy exchange (gain or loss) for a species s is given by

$$\frac{\partial W_s}{\partial t} = \frac{\partial}{\partial t} \int d^3\mathbf{x} \int dv \frac{1}{2} m_s v^2 f_s = \int d^3\mathbf{x} \int dv \frac{1}{2} m_s v^2 \frac{\partial f_s}{\partial t} \tag{1.28}$$

To make further progress, let us assume an equilibrium Maxwellian distribution for species s,

$$f_{s0} = \frac{n_0}{(2\pi)^{1/2} v_{ts}} e^{-v^2/2v_{ts}^2} \tag{1.29}$$

where $v_{ts}^2 \equiv T_s/m_s$ (note the absence of the factor of 2). Note that I am assuming two-component plasma with singly ionized ions and electrons so that $n_{0i} = n_{0e} \equiv n_0$. The total distribution function for species s is thereby given by

$$f_s(x,v,t) = f_{s0}(v) + \delta f_s(x,v,t). \tag{1.30}$$

We emphasize here that we have made *no ordering assumptions* on the magnitude of δf_s relative to f_{s0}, so the distribution described by this form is not limited in any way. The term δf_s contains the entire (nonlinear) perturbation, not just the lowest order (linear). Of course, the physical limitation

$$f_s(x,v,t) \geq 0 \tag{1.31}$$

must always be satisfied, so this means that $\delta f_s(x,v,t) \geq -f_{s0}(v)$ for all values of velocity v. Practically, this does lead to constraints on the allowable timestep in numerical simulations to maintain a physically realizable $f_s(x,v,t) \geq 0$ everywhere.

Now, let us write the Vlasov equation in terms of f_{s0} and δf_s,

$$\frac{\partial \delta f_s}{\partial t} = -v\frac{\partial \delta f_s}{\partial x} + \frac{q_s}{m_s}\frac{\partial \phi}{\partial x}\frac{\partial f_{s0}}{\partial v} + \frac{q_s}{m_s}\frac{\partial \phi}{\partial x}\frac{\partial \delta f_s}{\partial v}. \tag{1.32}$$

In this form, on the right-hand side, the first term is the ballistic term (linear), the second term is the linear wave-particle interaction term, and the third term is the nonlinear wave-particle interaction term. Next, we substitute the Vlasov equation into (1.28), yielding

$$\frac{\partial W_s}{\partial t} = \int d^3\mathbf{x}\int dv \frac{1}{2}m_s v^2 \frac{\partial f_s}{\partial t} = \int d^3\mathbf{x}\int dv \frac{1}{2}m_s v^2 \left[-v\frac{\partial \delta f_s}{\partial x} + \frac{q_s}{m_s}\frac{\partial \phi}{\partial x}\frac{\partial f_{s0}}{\partial v} + \frac{q_s}{m_s}\frac{\partial \phi}{\partial x}\frac{\partial \delta f_s}{\partial v}\right] \tag{1.33}$$

Here I will switch notation to 1D in space, replacing $d^3\mathbf{x}$ with dx (I'll make this consistent later, but to get the correct units for energy, it is important to do this carefully). Now we may evaluate the influence of each of these terms on the microscopic kinetic energy, W_s. We will discover that the first two terms are conservative (leading to no change in W_s), and only the third term leading to a net transfer of energy when integrated over the volume.

The first term may be written as a perfect differential,

$$\int dx \int dv \frac{1}{2}m_s v^2 \left[-v\frac{\partial \delta f_s}{\partial x}\right] = \int dx \frac{\partial}{\partial x}\left[\int dv \frac{1}{2}m_s v^2 \delta f_s\right] = 0 \tag{1.34}$$

so for periodic or infinite boundaries yields a zero value.

The second term may be written

$$\int dx \int dv \frac{1}{2}m_s v^2 \left[\frac{q_s}{m_s}\frac{\partial \phi}{\partial x}\frac{\partial f_{s0}}{\partial v}\right] = \int dx \frac{q_s}{2}\frac{\partial \phi}{\partial x}\left[\int dv \;\; v^2 \frac{\partial f_{s0}}{\partial v}\right] = 0. \tag{1.35}$$

Since we have chosen f_{s0} to be a Maxwellian (or if we choose f_{s0} to be *any* even function of v), then its derivative $\partial f_{s0}/\partial v$ is an odd function, so the integrand becomes an odd function evaluated over an even interval, yielding zero. Another way to see this is to replace evaluate the derivative as $\partial f_{s0}/\partial v = -(v/v_{ts}^2)f_{s0}$, leading to a velocity integral

$$-\int_{-\infty}^{\infty} dv \frac{v^3}{v_{ts}^2} f_{s0} = 0. \tag{1.36}$$

since, with f_{s0} even, the integrand is once again odd. Thus, we find that the second term contributes nothing to the change of W_s. In fact, this net contribution of zero does not even require an integration over the volume—the change of W_s due to this term must be zero everywhere in the domain.

Finally, we evaluate the third term.

$$\int dx \int dv \frac{1}{2} m_s v^2 \left[\frac{q_s}{m_s} \frac{\partial \phi}{\partial x} \frac{\partial \delta f_s}{\partial v} \right] = \int dx \frac{\partial \phi}{\partial x} \int dv \frac{q_s v^2}{2} \frac{\partial \delta f_s}{\partial v}. \tag{1.37}$$

For this term, because we have integrated over all velocity, we may perform an integration by parts in velocity to convert the velocity integral to

$$\int dv \frac{q_s v^2}{2} \frac{\partial \delta f_s}{\partial v} = \left[\frac{q_s v^2}{2} \delta f_s \right]_{-\infty}^{\infty} - \int dv \;\; q_s v \delta f_s = - \int dv \;\; q_s v \delta f_s \tag{1.38}$$

where the term in brackets is zero since $\lim_{v \to \pm\infty} \delta f_s(x, v) = 0$.

Putting all of this together, we obtain the following results for the rate of change of the different energies in the Vlasov-Poisson system:

$$\frac{\partial W_s}{\partial t} = - \int dx \frac{\partial \phi}{\partial x} \int dv \;\; q_s v \delta f_s = \int dx \;\; j_s E \tag{1.39}$$

$$\frac{\partial W_\phi}{\partial t} = \int dx \frac{\partial \phi}{\partial x} \left[\sum_s \int dv \;\; q_s v \delta f_s \right] = - \int dx \;\; jE \tag{1.40}$$

1.4.1 Implications for Linear vs. Nonlinear Energy Conservation

Note that linearization of the kinetic system leads to dropping the third term on the right-hand side of (1.33). But this is the only term that leads to a change in the energy of the particles W_s. So, although a linearized system will correctly describe the collisionless Landau damping of the electrostatic waves of the Vlasov-Poisson system, energy is *not* conserved in a linearized system. The nonlinear term, the third term on the right-hand side of (1.33), must be retained in order to achieve energy conservation. I have verified this using the simulation code I have written.

One thing that I need to work out in the electromagnetic case using gyrokinetics, is whether the nonlinearities kept in the nonlinear simulation runs are sufficient to achieve energy conservation. I think they must, since we can derive analytically the conserved free energy in the gyrokinetic case, but connecting that conserved free energy to the energy conservation forms I have derived here is somewhat tricky and will require substantial analytic work.

1.4.2 Diagnostics of the Energy Transfer to Particles

The rate of change of *microscopic kinetic energy* W_s for species s in the Vlasov-Poisson system is given by

$$\frac{\partial W_s}{\partial t} = - \int dx \frac{\partial \phi}{\partial x} \int dv \;\; q_s v \delta f_s = \int dx \;\; j_s E. \tag{1.41}$$

Note the velocity integration is performed over an even interval, so only the even component of the integrand will contribute to a non-zero value. Since the integrand is $q_s v \delta f_s$ it means that *only the odd component of the perturbed*

distribution function, $\delta f_{s\mathrm{odd}}$, contributes to a net change in the particle kinetic energy. Note the f_{s0} is chosen to be even, so it makes no contribution to the current, and therefore realizes no particle heating.

NOTE: To add a somewhat confusing point, in evaluating the energy of a particular fluctuation (which is an integral of v^2 times the distribution function over velocity), only the even component of f_s leads to a net energy.

Since we know that only $\delta f_{s\mathrm{odd}}$ in the third term contributes to a net change in particle energy (this is the resonant, or secular, transfer of energy from the fields to the particles), we can focus on what deviations that particular component generates in (x, v) phase space. In other words, we can investigate the energy change as a function of position or velocity.

Focusing on the idea of energy transfer as a function of position, note that the *microscopic particle kinetic energy* W_s is defined as a total energy, *i.e.*, an energy density integrated over the volume. But, the conversion of the change in particle energy to the form in (1.42) did not rely on the spatial integration (the integration by parts was performed in the velocity integral). Therefore, we should be able to view this rate of energy change as a function of position by evaluating

$$\frac{\partial W_s(x)}{\partial t} = -\frac{\partial \phi}{\partial x}\int dv \;\; q_s v \delta f_s = j_s(x)E(x). \tag{1.42}$$

Here it is important to realize that the ballistic term contribution to $\partial W_s/\partial t$ in (1.33) will not be zero at all points in space, but we know from this calculation that it yields no net energy transfer, so by looking at only the part of interest (given by the term above), we may obtain a cleaner signature.

Now, a perhaps even more important question is, "What perturbations to the distribution function δf_s are generated by the resonant energy transfer?" Rigorously, I believe we can take just $\delta f_{s\mathrm{odd}}$ and look at the change of δf_s due only to the third term on the right-hand side of (1.33), denoted $\delta f_{s\mathrm{wpi}}$. Thus, we have

$$\frac{\partial \delta f_{s\mathrm{wpi}}(x,v)}{\partial t} = -\frac{q_s}{m_s}\frac{\partial \phi(x)}{\partial x}\frac{\partial \delta f_{s\mathrm{odd}}(x,v)}{\partial v} = \frac{q_s}{m_s}E(x)\frac{\partial \delta f_{s\mathrm{odd}}(x,v)}{\partial v}, \tag{1.43}$$

[Am I missing a v^2 in the formula above?] where I explicitly included the dependencies of the variables on (x, v) phase space. *I think this is the true signature of resonant energy transfer from collisionless wave-particle interactions that we are ultimately seeking in this project.* Although rigorously we cannot convert to the following form without integrating over velocity (so that we can integrate by parts), we can also look at

$$\frac{\partial \delta f_{s\mathrm{wpi}}(x,v)}{\partial t} \simeq q_s v \delta f_s(x,v)E(x) \tag{1.44}$$

as a proxy for the more rigourous expression (1.43). Note, however, that this is the rate of change of particle energy, not just the rate of change of the distribution function.

Motivating the use of the the simpler expression (1.44) is the rate of change of energy of a charged particle in an electric field. The rate of change of energy (work done by the electric field) is given by

$$\frac{\partial W}{\partial t} = Fv \tag{1.45}$$

where the force of the electric field on the charge q is $F = qE$, so the rate of change of energy for the particle is

$$\frac{\partial W}{\partial t} = qvE. \tag{1.46}$$

The expression in (1.44) is simply an extension of this treatment for the rate of change of energy density for a collection of charged particles with the distribution δf_s. So there is good physical motivation here.

1.4.3 Ballistic Perturbation Gains No Energy

Let us now consider the results of this section in terms of the separation of the ballistic and wave components of the perturbed distribution function. Repeating the equations here, we split the perturbed distribution function into

$$\delta f_s = \delta f_{sB} + \delta f_{sW}. \tag{1.47}$$

where these two components evolve according to

$$\frac{\partial \delta f_{sB}}{\partial t} = -v\frac{\partial \delta f_{sB}}{\partial x} - v\frac{\partial \delta f_{sW}}{\partial x} \tag{1.48}$$

and

$$\frac{\partial \delta f_{sw}}{\partial t} = \frac{q_s}{m_s}\frac{\partial \phi}{\partial x}\frac{\partial f_{s0}}{\partial v} + \frac{q_s}{m_s}\frac{\partial \phi}{\partial x}\frac{\partial \delta f_{sB}}{\partial v} + \frac{q_s}{m_s}\frac{\partial \phi}{\partial x}\frac{\partial \delta f_{sW}}{\partial v}. \tag{1.49}$$

To estimate the energy gained by the perturbations in either of these components, multiply these equations by $m_s v^2/2$ and integrate over over all space (1D) and all velocity (1V) to obtain

$$\frac{\partial}{\partial t}\int dx \int dv \left(\frac{m_s v^2}{2}\delta f_{sB}\right) = -\int dx \frac{\partial}{\partial x}\left[\int dv \frac{m_s v^3}{2}(\delta f_{sB} + \delta f_{sW})\right] = 0. \tag{1.50}$$

Because the right-hand is a perfect differential, it integrates to zero for periodic or infinite boundary conditions. Therefore, it is clear that the ballistic perturbation of the distribution function δf_{sB} does not represent the effect resonant wave-particle interactions—it is a conservative term in the energy evolution of the particles.

What is not clear to me is whether the ballistic contribution to the wave perturbation (given by the second term on the right-hand side of (1.49)) yields a non-zero energy transfer. If there is a nonzero odd component to δf_{sB}, I believe it will contribute to the resonant energy transfer.

1.4.4 Relation to Field-Particle Correlations

The key now is to determine how measuring correlations can lead to a direct measure of the resonant energy transfer in wave-particle interactions.

One thing to note is that the rate of energy transfer to a species s is given by

$$\frac{\partial W_s}{\partial t} = -\int dx \frac{\partial \phi}{\partial x}\int dv \;\; q_s v \delta f_s = \int dx \;\; j_s E. \tag{1.51}$$

The integrand is the combination $q_s v \delta f_s(x,v)E(x)$, so correlations between $q_s v \delta f_s(x,v)$ and $E(x)$ are actually a direct measure of the rate of energy transfer. The normalized cross-correlation gives you the sign of this energy transfer, but the unnormalized cross-correlation actual gives you the the rate of energy density transfer (since it has not been intergrated over a volume, it is an a change of energy density rather than energy). Thus, although the normalized correlations

generate a strong signature of which particles are gaining energy and which particles are losing energy, the unnormalized version actual contains additional information in the unnormalized amplitude of the correlation. This unnormalized version will actually tell you which particles dominate the energy gain and loss.

I would predict, on physical grounds, the unnormalized signal should peak at the resonant velocity, with the largest energy gain just below the resonant velocity, and the largest loss just above. As you move away from the resonant velocity, this signal should taper off the zero (or something the oscillates rapidly, in space or time, but averages close to zero). How this will manifest in the presence of a broad spectrum of turbulent fluctuations requires significantly more thinking, but we can verify this idea using linear mode runs.

Another nice tool with the Vlasov-Poisson code that we can use is to compare these correlations with the linear and nonlinear terms. The linear term, which yields no resonant energy transfer to the particles, will still have correlation signal. If we can determine the difference in the two signals, perhaps we can devise a way to separate the two contributions so that can isolate the resonant energy transfer.

1.4.5 Note to Self

The 1D1V Nonlinear Vlasov Poisson code is an ideal tool for demonstrating unequivocally that Landau damping need not be spatially uniform. Ion-acoustic waves are probably the best choice for this demonstration (since in appropriate limits they are non-dispersive). I can initialize a localized ion acoustic wave perturbation, and compute directly the change of energy in the system as a function of position and time, showing that the heating occurs in particular regions, and not uniformly everywhere.

1.4.6 References on Wave-Particle Correlations in the Literature

Below, I summarize the details of the previous literature on wave-particle correlations:

1. Earliest work: Spiger et al. 1974, 1976—seems to be an electron beam injection experiment on a rocket.

2. **?** describes the instrumentation and **?** presents the results from a rocket flight, which are not terribly convincing. Electron count rates needed are too high, requiring a large opening angle detctor which smears out the signal.

3. **?** presents a coincidence study of electron-cyclotron harmonic (ECH) waves along with measured "pancake" distributions (electron distributions with electrons in the 100s eV range confined to a few degrees of 90°). The study **?** presents the electron distribution measurements.

4. **?** was the first paper to describe the development of wave-particle correlator instruments. In this case, it used an electron beam launched by a separated daughter payload, and measured phase-nbunching of this artificial electron beam due to the bunching. A companion instrument paper appears in **?**.

5. **?** uses GOES 1 and 2 spacecraft measurements of electrostatic cyclotron harmonic (ECH) emissions in the Earth's magnetosphere. This study finds of high ECH wave amplitudes (centered around the upper hybrid frequency) spatially coincident with measurements of the flux of field-aligned electrons at 100-200 eV (it is actually an anti-correlation that they find). This study is really just a correlation in space of regions of high wave spectral energy with low regions of fast parallel electrons.

6. **?** presents results modulation of electron measurements at twice the electron gyrofrequency in the auroral zone on a rocket.

7. **?** uses ground-based VLF receiver measurements of whistler-mode chorus, which sample around $L \sim 2 - 6$ and $\pm 20^\circ$ longitude and electron measurements from the geostationary ATS 6 satellite. Here temporal coincidence of whistler-mode chorus wave is associated with > 5 keV electrons at the synchronous altitude. Temporal coincidence. Ground wave and in situ electron coincidence.

8. **?** uses the Japanese EXOS-B satellite and VLF waves generated by a antenna at Siple station. Ground wave and in situ electron coincidence.

9. **?** presents measurements from an auroral sounding rocket of enhanced Langmuir waves and enhanced low energy (0.3-3.0 keV) electrons. The electrons are found to be bunched at the wave frequency during periods of intense Langmuir waves.

10. **?** presents theory applied to the above auroral sounding rocket measurements of electron bunching that showed Langmuir waves resoantly interacting with low-energy, field-aligned electrons.

11. **?** More detailed theory of wave-particle correlations and electron phase bunching for finite wavepackets of Langmuir waves.

12. **?** Nice description of wave-particle correlator instruments. They "look for periodicities in the input of a particle detector that match those of a component or components of the input of a wave detector." CRRES spacecraft

13. **?** describes the wave-particle correlator instrument on the FAST (Fast Auroral SnapshoT) spacecraft.

14. **?** presents rocket measurements of a new wave-particle correlator that smaples 16 times per expected wave period, yielding better resolution of the phase bunching of electron in the presence of strong Langmuir waves.

Other notes about wave-particle correlations in spacecraft measurements:

1. Note: These wave-particle correlation experiments do not differentiate counts of different particle as a function of velocity, but simply the total measurements particle flux in a window of energy and angle.

2. Groups doing wave-particle correlator instruments include Berkeley (Ergun), Sussex (Gough)

3. Wave-particle correlator instruments focus on the bunching of electrons with respect to wave phase, but do not study the variation in the correlation as a function of the particle velocity.

4. Add two Spiger references.

5. **?** estimates that electron bunching as only $\delta f/f \sim 2\%$ in the linear regime, so nonlinear effects are necessary to measure a signature of phase-bunching in space.

Chapter 2

Numerical Implementation of VP: Nonlinear Vlasov-Poisson Simulation Code

2.1 Overview of Code Implementation

2.2 Vlasov-Poisson Problem

The 1D-1V Vlasov-Poisson system is governed by the Boltzmann equation for the species distribution functions $f_s(x, v, t)$

$$\frac{\partial f_s}{\partial t} + v\frac{\partial f_s}{\partial x} - \frac{q_s}{m_s}\frac{\partial \phi}{\partial x}\frac{\partial f_s}{\partial v} = 0 \tag{2.1}$$

and the Poisson equation for the scalar electrostatic potential $\phi(x, t)$

$$\frac{\partial^2 \phi}{\partial x^2} = -4\pi \sum_s \int_{-\infty}^{+\infty} dv \quad q_s f_s \tag{2.2}$$

Two critical separations are performed to yield the most insightful decomposition of the time evolution, as described in the next two subsections.

2.2.1 Separating Linear and Nonlinear Terms

The species distribution function $f_s(x, v, t)$ is seperated into a time-invariant, spatially uniform equilibrium part $f_{s0}(v)$ and a perturbation $\delta f_s(x, v, t)$,

$$f_S(x, v, t) = f_{s0}(v) + \delta f_S(x, v, t) \tag{2.3}$$

Note that *no ordering is assumed* about the magnitude of $\delta f_s(x, v, t)$ relative to $f_{s0}(v)$, so this yields an unconstrained nonlinear evolution. Of course, the full solution is physically required to have $f_S(x, v, t) \geq 0$ (the distribution function can never become negative), and practically this will require a limitation on the allowable timestep depending on the

amplitude of the perturbation, so that the total distribution function never becomes negative at any point (x, v). This decomposition yields a Boltzmann equation of the form

$$\frac{\partial \delta f_s}{\partial t} = -v\frac{\partial \delta f_s}{\partial x} + \frac{q_s}{m_s}\frac{\partial \phi}{\partial x}\frac{\partial f_{s0}}{\partial v} + \frac{q_s}{m_s}\frac{\partial \phi}{\partial x}\frac{\partial \delta f_s}{\partial v}, \tag{2.4}$$

where the first term on the left-hand side is the (linear) ballistic term, the second term describe linear wave-particle interactions, and the third term represents nonlinear corrections to the wave-particle interaction. As we shall see, keeping the nonlinear wave-particle interaction term is necessary to achieve conservation of energy as field energy is transferred to the particles via collisionless wave-particle interactions.

2.2.2 Separating Ballistic and Wave Terms

Since the Boltzmann equation (3.9) is linear in δf_s, we can perform an operator splitting to separate the perturbation of the distribution function due to the ballistic term δf_{sB} and the perturbation due to the wave-particle interaction terms δf_{sW}, where the total perturbation is given by

$$\delta f_s = \delta f_{sB} + \delta f_{sW}. \tag{2.5}$$

The equations describing the evolution of each of these components are

$$\frac{\partial \delta f_{sB}}{\partial t} = -v\frac{\partial \delta f_{sB}}{\partial x} - v\frac{\partial \delta f_{sW}}{\partial x} \tag{2.6}$$

and

$$\frac{\partial \delta f_{sw}}{\partial t} = \frac{q_s}{m_s}\frac{\partial \phi}{\partial x}\frac{\partial f_{s0}}{\partial v} + \frac{q_s}{m_s}\frac{\partial \phi}{\partial x}\frac{\partial \delta f_{sB}}{\partial v} + \frac{q_s}{m_s}\frac{\partial \phi}{\partial x}\frac{\partial \delta f_{sW}}{\partial v}. \tag{2.7}$$

Here the evolution of the ballistic component is completely linear, and the evolution of the wave component has a linear term and two nonlinear terms.

2.3 Green's Function Solution for Electrostatic Potential

[More detail to be filled in.]

The Green's Function solution to the linear, inhomogeneous, second-order differential equation

$$\frac{\partial^2 \phi}{\partial x^2} = f(x) \tag{2.8}$$

with periodic boundary conditions $\phi(-L) = \phi(L)$ is given by

$$G(x, x') = \begin{cases} (-1/2L)(L + x')(L - x) & -L \le x' < x \\ (-1/2L)(L + x)(L - x') & x < x' \le L \end{cases} \tag{2.9}$$

The solution for the electrostatic potential is given by

$$\phi(x) = \int_{-L}^{L} G(x', x) f(x') dx' \tag{2.10}$$

Quantity	Normalization	Quantity	Definition
Position	$\hat{x} = x/\lambda_{de}$	Debye Length	$\lambda_{de}^2 = T_e/4\pi n_0 q_e^2$
Velocity	$\hat{v}_s = v/v_{ts}$	Thermal Velocity	$v_{ts}^2 = T_s/m_s$
Time	$\hat{t} = \omega_{pe} t$	Plasma Frequency	$\omega_{pe}^2 = 4\pi n_0 q_e^2/m_e$
Potential	$\hat{\phi} = q_e\phi/T_e$		
Distribution	$\hat{f}_{s0} = f_{s0} v_{ts}/n_0$		

Table 2.1: Dimensionless normalization of quantities and definitions of plasma parameters in cgs units. The Boltzmann constant is absorbed into temperature, giving temperature in units of energy.

where the inhomogenous source term is $f(x) = -4\pi\rho(x) = -4\pi \sum_s \int dv\ q_s f_s$. This solution may be written

$$\phi(x) = \frac{2\pi}{L}\left\{(L-x)\int_{-L}^{x}(L+x')\rho(x')dx' + (L+x)\int_{x}^{L}(L-x')\rho(x')dx'\right\} \tag{2.11}$$

The numerical implementation of this Green's function solution is

$$I_{-L}(x) = \int_{-L}^{x}(L+x')\rho(x')dx' \tag{2.12}$$

$$I_{+L}(x) = \int_{x}^{L}(L-x')\rho(x')dx' \tag{2.13}$$

$$\phi(x) = \frac{2\pi}{L}\left\{(L-x)I_{-L}(x) + (L+x)I_{+L}(x)\right\} \tag{2.14}$$

where the charge density is computed by

$$\rho(x) = \sum_s \int dv\ q_s f_s \tag{2.15}$$

We may also write the electric field as

$$E(x) = -\frac{\partial\phi}{\partial x} = \frac{2\pi}{L}\left\{I_{-L}(x) - I_{+L}(x)\right\} \tag{2.16}$$

2.4 Normalization

Below I outline the normalizations for the code, also presented concisely in Table 2.1.

Note that the electrostatic potential ϕ is normalized in terms of the electron charge, so its sign is opposite of what you would normally expect.

$$\hat{\phi} = \frac{q_e\phi}{T_e} \tag{2.17}$$

$$\hat{x} = \frac{x}{\lambda_{de}} \tag{2.18}$$

$$\hat{t} = t\omega_{pe} \tag{2.19}$$

$$f_{s0} = \frac{n_0}{(2\pi)^{1/2} v_{ts}} e^{-v^2/2v_{ts}^2} \tag{2.20}$$

$$\hat{f}_{s0} = \frac{f_{s0}}{n_0/v_{ts}} \tag{2.21}$$

$$v_{te} = \lambda_{de}\omega_{pe} \tag{2.22}$$

Note that velocity is defined in terms of the species thermal velocity. Velocity grids in the code are defined for each species in terms of the thermal velocity *for that species*. Thus, in terms of the species normalized velocity, they are the same.

$$\hat{v}_s = \frac{v}{v_{ts}} \tag{2.23}$$

NOTE: The definition of the thermal velocity for the Vlasov-Poisson problem does not have the 2 in it,

$$v_{te}^2 = \frac{T_e}{m_e} \tag{2.24}$$

$$\omega_{pe}^2 = \frac{4\pi n_0 q_e^2}{m_e} \tag{2.25}$$

$$\lambda_{de}^2 = \frac{T_e}{4\pi n_0 q_e^2} \tag{2.26}$$

$$v_{te} = \lambda_{de}\omega_{pe} \tag{2.27}$$

Zero net charge

$$n_{0e} = n_{0i} \equiv n_0 \tag{2.28}$$

Assume a singly ionized plasma

$$q_e = -q_i \tag{2.29}$$

The linear dispersion relation is computed in terms of the dimensionless parameters $\overline{\omega} = \frac{\omega}{\omega_{pe}}(k\lambda_{de}, T_i/T_e, m_i/m_e)$.

The normalized Boltzmann equation for electrons

$$\frac{\partial \hat{f}_e}{\partial \hat{t}} + \hat{v}_e \frac{\partial \hat{f}_e}{\partial \hat{x}} - \frac{\partial \hat{\phi}}{\partial \hat{x}} \frac{\partial \hat{f}_e}{\partial \hat{v}_e} = 0 \tag{2.30}$$

The normalized Boltzmann equation for ions

$$\frac{\partial \hat{f}_i}{\partial \hat{t}} + \left(\frac{T_i}{T_e}\frac{m_e}{m_i}\right)^{1/2} \hat{v}_i \frac{\partial \hat{f}_i}{\partial \hat{x}} - \frac{q_i}{q_e}\left(\frac{T_e}{T_i}\frac{m_e}{m_i}\right)^{1/2} \frac{\partial \hat{\phi}}{\partial \hat{x}} \frac{\partial \hat{f}_i}{\partial \hat{v}_i} = 0 \tag{2.31}$$

2.4.1 Energy Diagnostic Normalization

2.5 Notes on VP2 (Multispecies and drifts) and VP3 (Krook Collisions) Implementation

1. The species properties (temperatures, masses, charges, densities, drifts, collision frequencies) are all included in a data structure of type `specie` (defined in `vp_data.f90`. In this data structure, there is also a logical flag `P_s` to turn off any initial perturbation in that species.

2. Note that the use of a data structure here is probably not optimal. Access to data structures is slow, and species dependent factors appear in the innermost loop of the calculations, likely slowing down the performance substantially.

3. The output file `runname.test_phi` write out an array of $x, \phi(x), d\phi(x)/dx, d^2\phi(x)/dx^2, \rho$ to test the Green's function solver for the potential$\phi(x)$ as a function of the charge density $\rho(x)$. Whether this output file is written is hard-coded with alogical flag, and is general .false. Change it to .true. and re-compile to output this file for testing.

2.6 Numerical Discretization

2.6.1 3rd-Order Adams-Bashforth Timestepping

For an equation given by

$$\frac{\partial y}{\partial t} = g, \tag{2.32}$$

the 3rd-Order Adams-Bashforth scheme uses

$$y^{n+1} = y^n + \frac{\Delta t}{12}\left[23g^n - 16g^{n-1} + 5g^{n-2}\right] \tag{2.33}$$

To bootstrap up to having enough time derivatives to start timestepping by this scheme, we use a combination of one first order Eulerian timestep with step size $\Delta t/32$, followed by 6 second-order leapfrog timesteps, each jumping from $t = 0$, such that the fifth timestep yields the result at $t = \Delta t$ and the sixth timestep yields the result at $t = 2\Delta t$. The time derivative at the sixth timestep is saved (which is calculated at $t = \Delta t$ along with the initial time derivative at $t = 0$ to yield the $(n-1)$ and $(n-2)$ time derivatives needed by the Adams-Bashforth scheme.

2.6.2 Spatial and Velocity Derivatives

Spatial derivatives are second-order centered finite-difference

$$\frac{\partial y}{\partial x} = \frac{y_{i+1} - y_{i-1}}{2\Delta x} \tag{2.34}$$

with periodic wrapping at the boundary in x.

Velocity space derivatives are also second-order centered finite-difference

$$\frac{\partial f}{\partial v} = \frac{f_{j+1} - f_{j-1}}{2\Delta v} \tag{2.35}$$

except at the extremal velocity points which just use first-order differencing

$$\frac{\partial f}{\partial v} = \frac{f_j - f_{j-1}}{\Delta v} \tag{2.36}$$

2.7 Initial Conditions

Here I describe the various types of initial conditions that are implemented in `VP`.

A significant restriction on the initial condition of the code is that the net charge density must be zero, $\sum_s n_s = 0$. This is necessary so that the Green's Function solution for the electrostatic potential with periodic boundary conditions is correct. A non-zero net charge density will yield an erroneous solution for the electrostatic potential.

2.7.1 Initialization of Electron Density Perturbation

The option `ic=1` initializes a spatial density perturbation in the electrons, where distribution remains Maxwellian everywhere but is modulated in amplitude to yield an electron density perturbation with wavenumber k that has spatial amplitude variation $\delta n \sin(kx)$.

This initial condition nicely generates a pair of counterpropagating Langmuir waves that generate a standing wave pattern. The frequency and damping rate of the resulting standing wave agrees with that of a Langmuir wave with the same $k\lambda_{de}$. Note that the Langmuir wave frequency (2.37) and damping rate (2.38) are insenstive to the parameters T_i/T_e and m_i/m_e. A plot of the results from linear runs of `VP` compared to the solutions of the linear Vlasov-Poisson dispersion relation and the analytical estimates in Section (2.7.2) are shown in Figure 2.1.

2.7.2 Linear Wave Eigenfunction

For Langmuir waves in a plasma (in the limit $\omega/k \gg v_{te}$), the real frequency and damping rate are estimated by

$$\omega_r^2 = \omega_{pe}^2 \left(1 + 3k^2\lambda_{de}^2\right) \tag{2.37}$$

$$\gamma = -\sqrt{\frac{\pi}{8}} \frac{\omega_{pe}}{|k\lambda_{de}|^3} \exp - \left(\frac{1}{2k^2\lambda_{de}^2} + \frac{3}{2}\right) \tag{2.38}$$

For in acoustic waves (in the limit $v_{ti} \ll \omega/k \ll v_{te}$), the real frequency and damping rate are estimated by

$$\omega_r^2 = \frac{k^2 C_s^2}{1 + k^2\lambda_{de}^2} \tag{2.39}$$

$$\gamma = -\sqrt{\frac{\pi}{8}} \frac{|\omega_r|}{(1 + k^2\lambda_{de}^2)^{3/2}} \left[\left(\frac{T_e}{T_i}\right)^{3/2} \exp\left(-\frac{T_e/T_i}{2(1 + k^2\lambda_{de}^2)}\right) + \sqrt{\frac{m_e}{m_i}}\right] \tag{2.40}$$

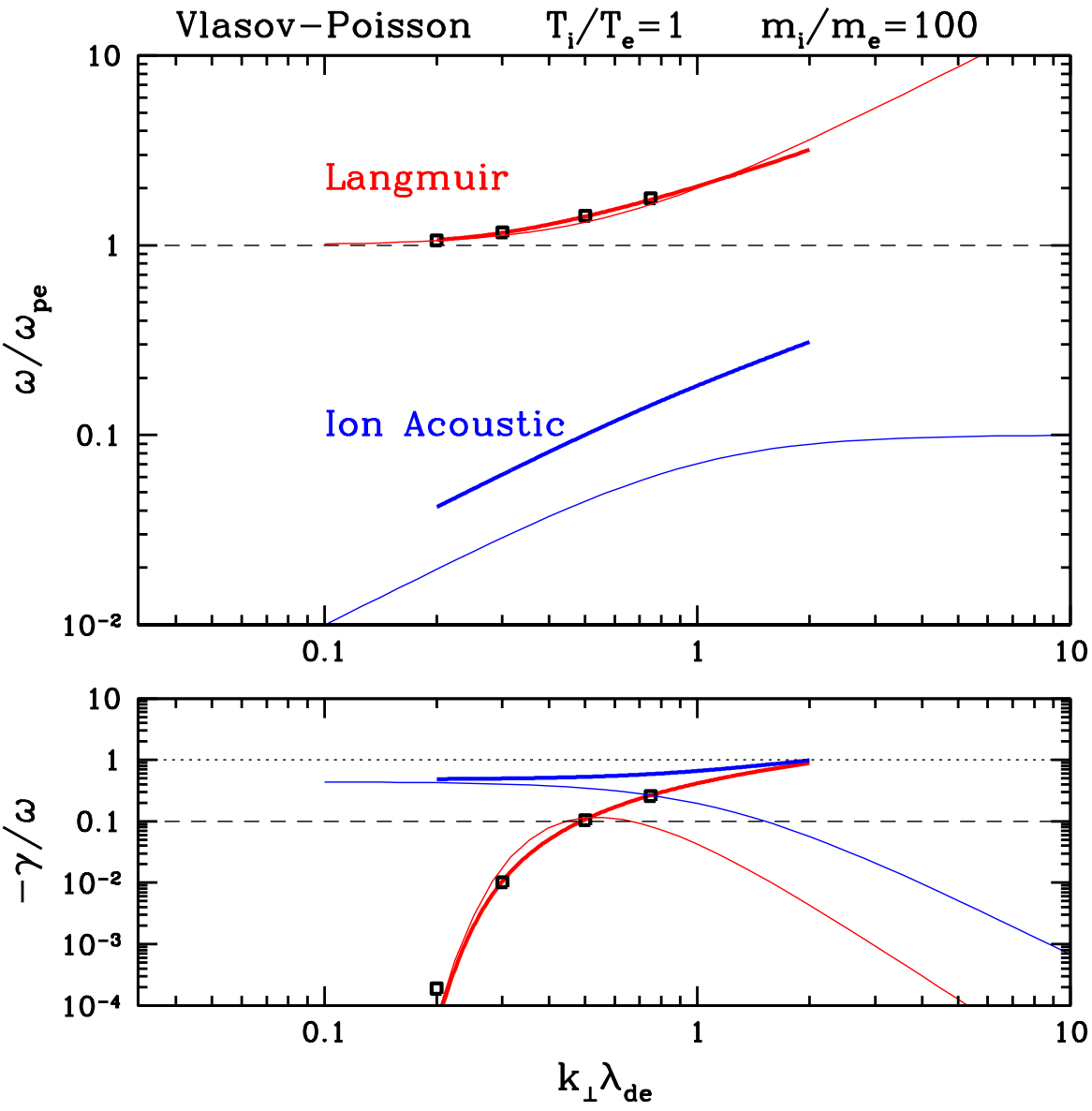

Figure 2.1: Validation of electron density initialization for Langmuir wave frequency and dmaping rate using the Vlasov-Poisson simulation code `VP`. For Langmuir (red) and ion acoustic (blue) waves, we show numerical solutions of the linear Vlasov-Poisson dispersion relation from `waves` (thick lines), the analytical estimates from Section (2.7.2) (thin lines), and the numerical simulation results from `VP` using electron density fluctuation initialization (black boxes). Parameters for this case are $\tau = T_i/T_e = 1$ and $\mu = m_i/m_e = 100$.

where the ion acoustic sound speed is given by

$$C_s^2 = \frac{T_e}{m_i}. \tag{2.41}$$

Calculation for Distribution Eigenfunction

Beginning with the linearized 1D Vlasov Equation for electrostatic fluctuations,

$$\frac{\partial f_{1s}}{\partial t} + v\frac{\partial f_{1s}}{\partial x} - \frac{q_s}{m_s}\frac{\partial \phi}{\partial x}\frac{\partial f_{0s}}{\partial v} = 0 \tag{2.42}$$

we Fourier transform in space and time, thus assuming that the distribution function has the form

$$f_{1s}(x, v, t) = \tilde{f}_{1s}(k, v)e^{i(kx-\omega t)} \tag{2.43}$$

and the electrostatic potential has the form

$$\phi_1(x, t) = \tilde{\phi}_1(k)e^{i(kx-\omega t)}, \tag{2.44}$$

and solve for $\tilde{f}_{1s}(k, v)$, yielding

$$\tilde{f}_{1s}(k, v) = -\frac{q_s}{m_s}\frac{k\tilde{\phi}_1}{\omega - kv}\frac{\partial f_{0s}}{\partial v} \tag{2.45}$$

Taking the equilibrium distribution function to be a Mawellian,

$$f_{0s} = \frac{n_0}{(2\pi)^{1/2}v_{ts}}e^{-v^2/2v_{ts}^2} \tag{2.46}$$

the velocity derivative of f_{0s} is given by

$$\frac{\partial f_{0s}}{\partial v} = -\frac{v}{v_{ts}^2}f_{0s}. \tag{2.47}$$

Using this, we can simplify the solution for $\tilde{f}_{1s}(k, v)$ to

$$\tilde{f}_{1s}(k, v) = \left(\frac{q_s\tilde{\phi}_1}{T_s}\right)\frac{kv}{\omega - kv}f_{0s} \tag{2.48}$$

Since the perturbed distribution function $f_{1s}(x, v, t)$ must be real, then the the Fourier transform of the distribution function $\tilde{f}_{1s}(k, v)$ must satisfy a reality condition

$$\tilde{f}_{1s}(-k, v) = \tilde{f}_{1s}^*(k, v). \tag{2.49}$$

Thus the initial condition for $f_{1s}(x, v, t)$ at $t = 0$ is given by

$$f_{1s}(x, v, 0) = \frac{1}{2}\left(\tilde{f}_{1s}(k, v)e^{ikx} + \tilde{f}_{1s}^*(k, v)e^{-ikx}\right) = \mathrm{Re}\left[\tilde{f}_{1s}(k, v)e^{ikx}\right] \tag{2.50}$$

Normalizaton of the Distribution Eigenfunction

Employing the code normalization outlined in Section (2.4), we obtain the following general result for the initial perturbed distribution function $f_{1s}(x, v, 0)$,

$$\left(\frac{v_{ts} f_{1s}(x, v, 0)}{n_0}\right) = \mathrm{Re}\left[\left(\frac{v_{ts}\tilde{f}_{1s}(k, v)}{n_0}\right) e^{ik\lambda_{de}\hat{x}}\right] \tag{2.51}$$

where $\hat{x} = x/\lambda_{de}$. The normalized, Fourier transform of the distribution function is given by

$$\left(\frac{v_{ts}\tilde{f}_{1s}(k, v)}{n_0}\right) = \frac{q_s}{q_e}\frac{T_e}{T_s}\left(\frac{q_e\tilde{\phi}_1}{T_e}\right)\frac{k\lambda_{de}\hat{v}_s\left(\frac{T_s}{T_e}\frac{m_e}{m_s}\right)^{1/2}}{(\omega/\omega_{pe}) - k\lambda_{de}\hat{v}_s\left(\frac{T_s}{T_e}\frac{m_e}{m_s}\right)^{1/2}}\left(\frac{v_{ts} f_{0s}}{n_0}\right) \tag{2.52}$$

where $\hat{v}_s = v/v_{ts}$. Using $q_e = -q_i$, $\tau = T_i/T_e$, and $\mu = m_i/m_e$ to simplify the notation, we find the follow results for the electrons and ions

$$\left(\frac{v_{te}\tilde{f}_{1e}(k, v)}{n_0}\right) = \left(\frac{q_e\tilde{\phi}_1}{T_e}\right)\frac{k\lambda_{de}\hat{v}_e}{(\omega/\omega_{pe}) - k\lambda_{de}\hat{v}_e}\left(\frac{v_{te} f_{0e}}{n_0}\right) \tag{2.53}$$

$$\left(\frac{v_{ti}\tilde{f}_{1i}(k, v)}{n_0}\right) = -\frac{1}{\tau}\left(\frac{q_e\tilde{\phi}_1}{T_e}\right)\frac{k\lambda_{de}\hat{v}_i\left(\tau/\mu\right)^{1/2}}{(\omega/\omega_{pe}) - k\lambda_{de}\hat{v}_i\left(\tau/\mu\right)^{1/2}}\left(\frac{v_{ti} f_{0i}}{n_0}\right) \tag{2.54}$$

These are the normalized equations that are coded into the eigenfunction initialization in `VP`.

2.7.3 Localized Wavepacket

[Not yet implemented]

A simple way to implement a spatial localized wavepacket while maintaining the required net charge density of zero is to use a perturbation that is odd about the center of the domain and window the waveform with an exponential (or any other desired window) evenly about the center of the domain.

Doing a localized wavepacket will enable us to see a propagating wave even with a simple density perturbation initialization (rather than having to initialize an exact linear eigenfunction).

2.8 Notes

1. Splitting the ballistic and wave terms, our initial perturbation will be *all* in the wave term, with $\delta f_{eB}(x, v, 0) = 0$.

2. I need to implement collisions to keep velocity space resolved in the nonlinear simulations.

3. This numerical solver should help me to determine what nonlinear physical effects are included in the NL GK simulations, and which are missing.

4. IMPORTANT NOTE: The potential is normalized by

$$\hat{\phi} = \frac{q_e \phi}{T_e}$$

and since $q_e < 0$, this means that the normalized potential $\hat{\phi}$ has the opposite sign from ϕ, a point which could very easily lead to confusion.

Chapter 3

Results for Landau Damping from VP: Nonlinear Vlasov-Poisson Simulation Code

3.1 Two Test Cases

Weakly Damped Case

It is important, for weakly damped cases to be properly modeled, that range of velocity space simulated includes the resonant velocity, $v_{max} > \omega/k$. If not, the damping is not properly resolved (in a linear run, the damping rate is too low). Note also that, for weakly damped cases, nonlinear runs effectively have no damping at all. The reason is that a run is weakly damped (for Langmuir waves, specifically) if the resonant velocity is far out in the tail of the electron distribution function. Thus, it takes very little energy from the wave to flatten that part of the distibution function. This is demonstrated in Figure 3.9 below.

For the weakly damped case, we take the following plasma and numerical parameters:

$k\lambda_{de} = 0.2$

$\omega_r/\omega_{pe} = 1.06$

$\gamma/\omega_{pe} = -4.99 \times 10^{-5}$

n_x	n_v	v_{max}	n_L	NL	μ	τ	cfl	N_t	n_t out	δn	n_{k1}
128	256	8	5	T	100	1	0.25	5000	100	0.025	1

Note that this run becomes numerically unstable at $t > 220$, but this is much longer than we need (it is more than 30 Langmuir wave periods). Reducing `cfl` would delay or cure the computational instability.

This run has effectively no damping of the Langmuir wave, $\gamma = 0$, because wave-particle interactions very easily flatten out the distribution function in the neighborhood of the resonant velocity, as demonstrated in Figure 3.9 below.

With a reduced `cfl`= 0.0625, the perturbed energy is conserved to about 0.4%.

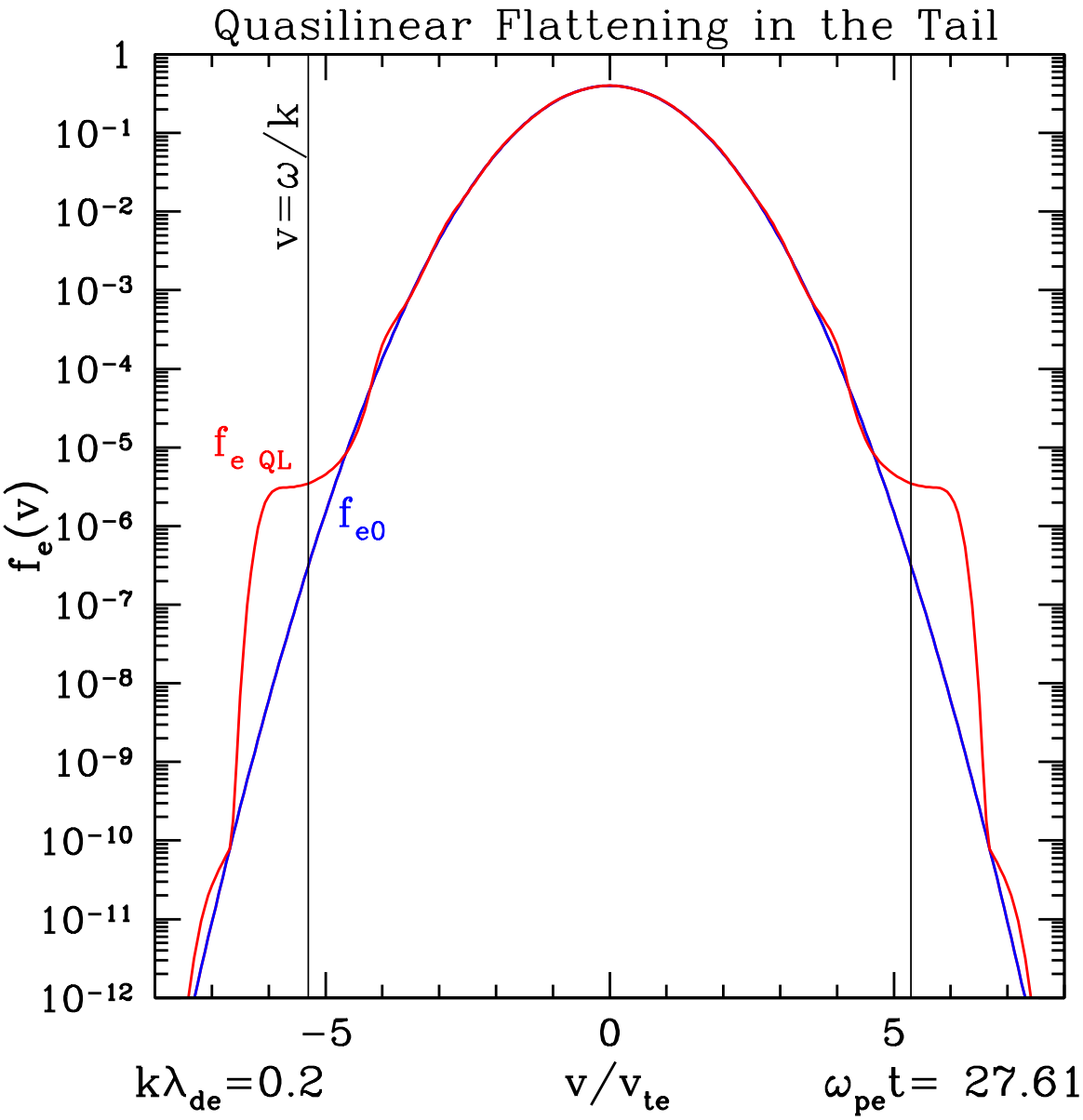

Figure 3.1: For a Langmuir wave simulation (initialized with a spatial electron density perturbation) with plasma parameters $k\lambda_{de} = 0.2$, $\tau = T_i/T_e = 1$, and $\mu = m_i/m_e = 100$. Logarithmically plotted are the equilibrium electron distribution function f_{e0} (blue) and the quasilinear (averaged over x) total electron distribution function f_{eQL} (red) at time $\omega_{pe}t = 27.61$. For a frequency $\omega/\omega_{pe} = 1.06$, the resonant phase velocity is $v/v_{te} = 5.3$, indicated by the vertical black lines.

Moderately Damped Case

Moderately Damped:
$k\lambda_{de} = 0.5$
$\omega_r/\omega_{pe} = 1.43$
$\gamma/\omega_{pe} = -1.59 \times 10^{-1}$

n_x	n_v	v_{max}	n_L	NL	μ	τ	cfl	N_t	n_t out	δn	n_{k1}
128	256	5	2	T	100	1	0.25	10000	100	0.1	1

Observations:

1. This run appears to yield a good evolution (at least up to $\hat{t} = 49$) without $f_e < 0$ anywhere, and energy conservation is very good.
2. No nonlinear echo behavior up to $t = 49$, although the exponential decay of field energy appears to be arrested around $t = 25$.
3. The ballistic structure develops relatively slowly relative to the timescale of the Landau damping. In this case, the field energy is largely completely gone by $\hat{t} = 18$.
4. The overall odd oscillation in δf_{ew} is due to the wave oscillation behavior, and varies sinusoidally in space. What remains is the quasilinear version of the perturbation when averaged over space.
5. Note, although the δf_{ew} looks even, perhaps the field changes sign and so the signature is heating/damped is thereby the same on both sides?
6. Question: Is a spatial average possible before computing the energy by velocity integration? If so, then the quasilinear pieces of the distribution function tell you about the total change in the distribution function.
7. Note that δf_{ewQL} in Figure 3.8 looks exactly even in v, meaning that the energy transfer will be exactly odd as needed (no need here to separate even and odd!).

3.2 Identification through Correlations

In this section I outline ideas on how to identify the signature of Landau damping through correlations.

1. For weakly damped runs, the normalized correlations will show a signature at the phase velocity way out in the tail. But the unnormalized correlations will see basically nothing. For real spacecraft measurements, the small correlated fluctuations in the tail will probably not be possible to observe (which is not a problem, since there is little damping happening).
2. The key problem is to separate the oscillating energy transfer between particles and fields due to a wave from the secular energy transfer due resonant wave-particle interactions. The correlations may help with this, because the net energy transfer is a wave is zero, so if the signal is averaged over a few wave periods, the oscillating wave energy

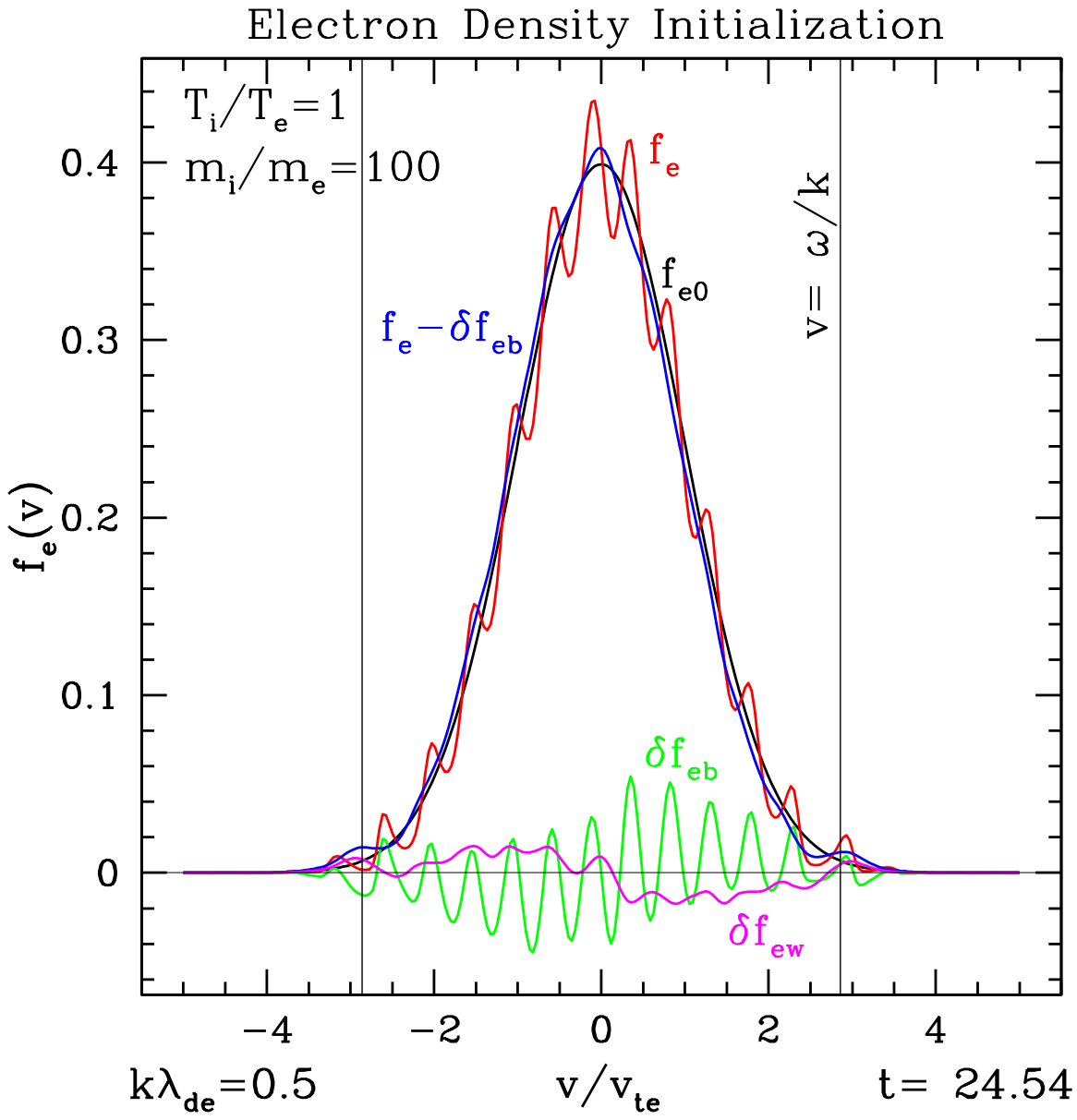

Figure 3.2: The evolution of the electron distribution function due to the Landau damping of a standing Langmuir wave pattern initialized by a sinusoidal electron density perturbation in a plasma with $\tau = T_i/T_e = 1$ and $\mu = m_i/m_e = 100$. Plotted are the equilibrium f_{e0} (black), total f_e (red), ballistic perturbation δf_{eb} (green), wave perturbation δf_{ew} (magenta), and $f_e - \delta f_{eb}$ (blue). Quasilinear flattening is observed at the resonant velocities $v_p/v_{te} = \pm(\omega/\omega_{pe})/(k\lambda de) = \pm 2.83$ (vertical black lines)

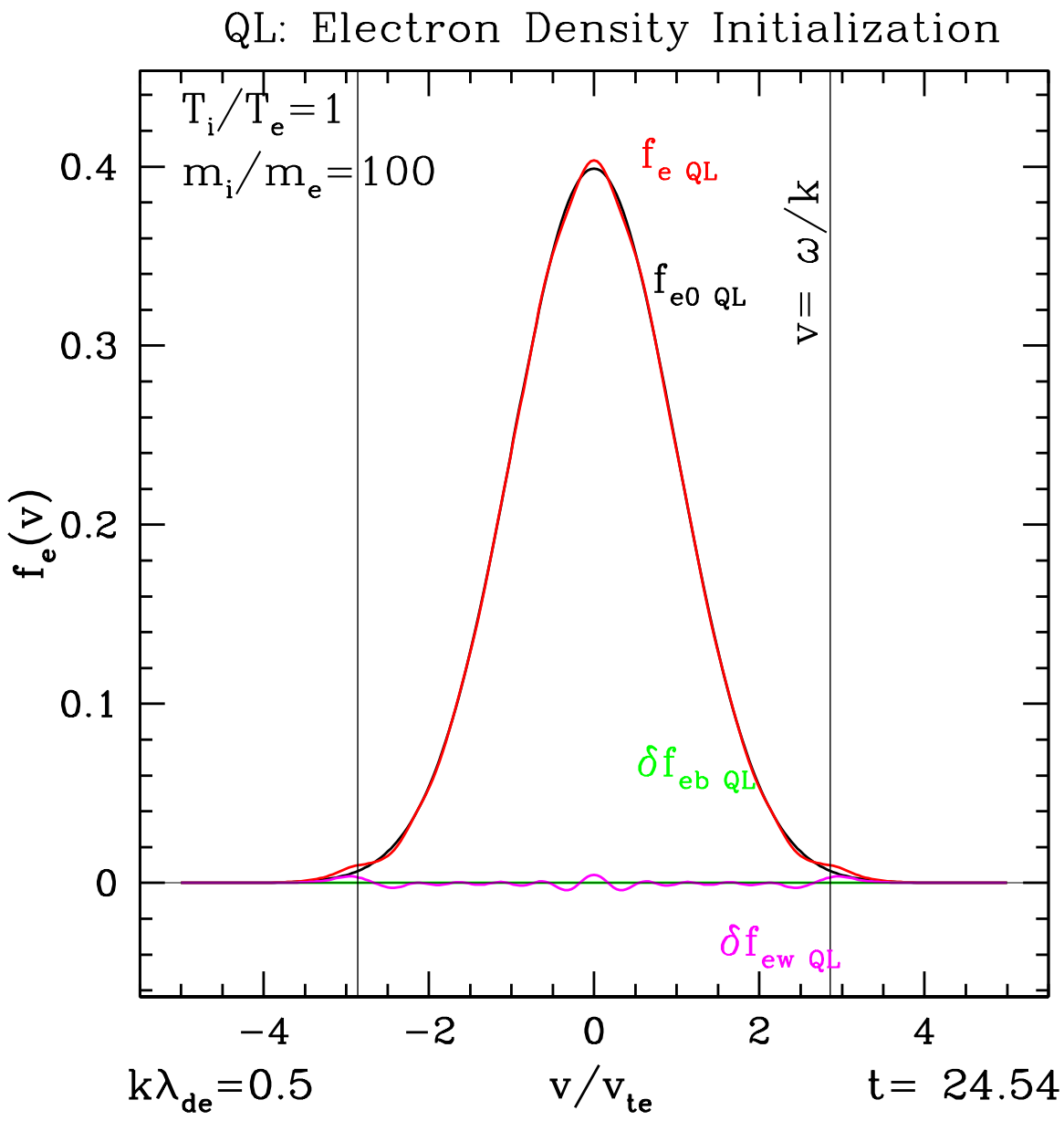

Figure 3.3: The quasilinear evolution of the electron distribution function due to the Landau damping of a standing Langmuir wave pattern initialized by a sinusoidal electron density perturbation in a plasma with $\tau = T_i/T_e = 1$ and $\mu = m_i/m_e = 100$. Plotted are the quasilinear (x-averaged) value for the equilibrium f_{e0QL} (black), total f_{eQL} (red), ballistic perturbation δf_{ebQL} (green), and wave perturbation δf_{ewQL} (magenta). Quasilinear flattening is observed at the resonant velocities $v_p/v_{te} = \pm(\omega/\omega_{pe})/(k\lambda de) = \pm 2.83$ (vertical black lines)

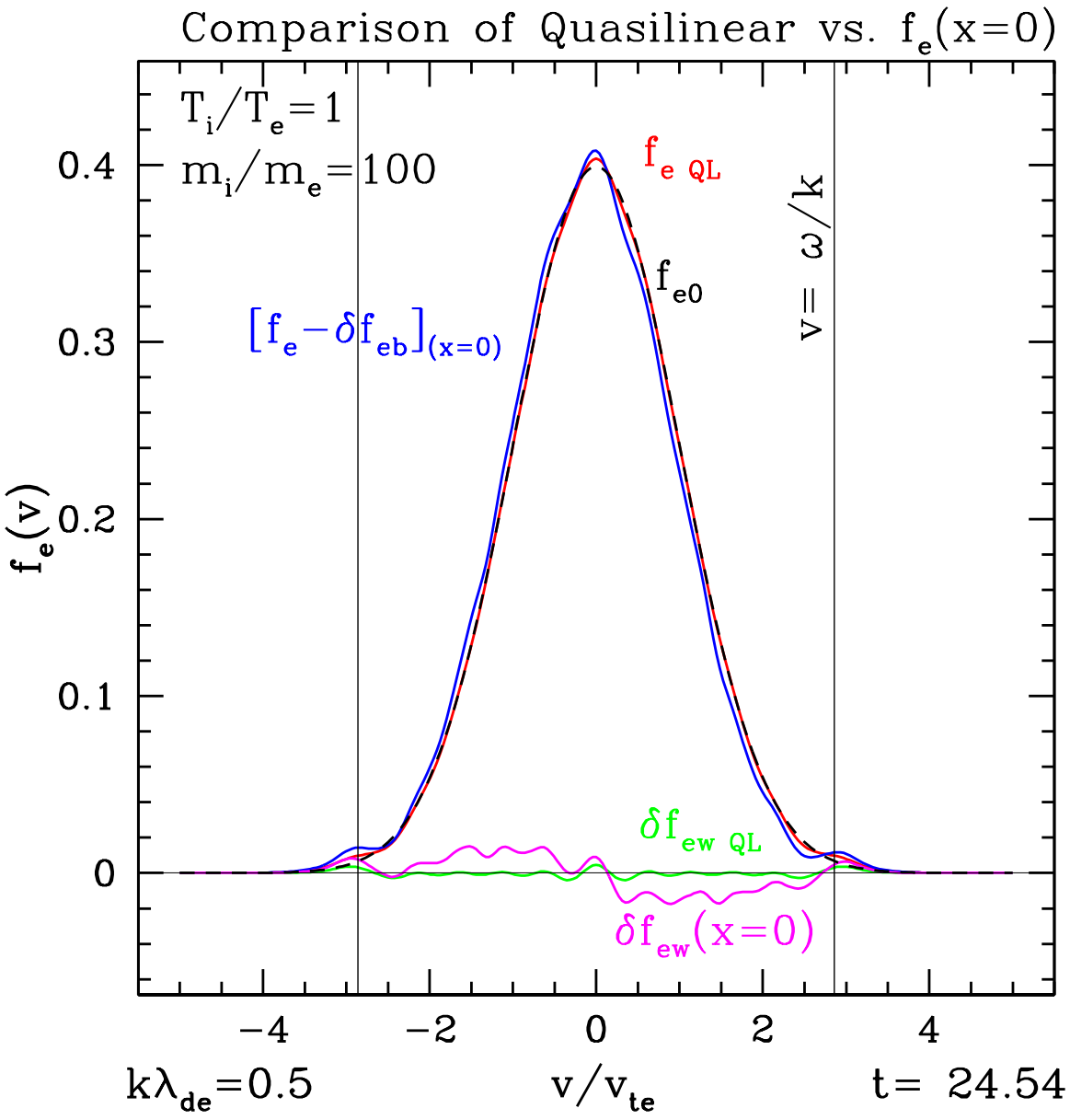

Figure 3.4: Comparison of the quasilinear evolution of the electron distribution function due to the Landau damping of a standing Langmuir wave pattern with the electron distribution function at a particular position in space, $x = 0$. Plasma parameters are $\tau = T_i/T_e = 1$ and $\mu = m_i/m_e = 100$. Plotted are the equilibrium f_{e0} (black), quasilinear f_{eQL} (red), $f_e(x = 0)$ (blue), quasilinear wave perturbation δf_{ewQL} (green), and wave perturbation $\delta f_{ew}(x = 0)$ (magenta). Quasilinear flattening is observed at the resonant velocities $v_p/v_{te} = \pm(\omega/\omega_{pe})/(k\lambda de) = \pm 2.83$ (vertical black lines)

transfer averages out. However, the secular energy transfer due to Landau damping should add constructively. So, even if the amplitude of the secular energy transfer due to Landau damping is very small, we may be able to distinguish it from the oscillating wave energy transfer of much larger amplitude.

3. The phase relationship between the wave fields and wave δf may also differ from the phase relationship between the wave fields and resonant particles. This may also turn out to be a valuable quantity to measure and plot.

   For example, for a wave on a string, when the kinetic energy is maximum (when the string is straight), the restoring force is zero. When the restoring force is maximum, the kinetic energy is zero. Thus, these two quantities should be phase-shifted from each other by $\pi/2$. We may be able to see this if we compare the right quantities analogous to kinetic energy and restoring force for our system.

3.3 Numerical Recurrence in Linear Run

As detailed in **?**, numerical recurrence of the initial conditions can occur for linear (or nonlinear) runs due to the limited velocity space resolution. The recurrence time is given by

$$T_{rec} = \frac{2\pi}{k\Delta v} \tag{3.1}$$

Normalized in our code units, this becomes

$$\omega_{pe} T_{rec} = \frac{2\pi}{k\lambda_{de}(\Delta v/v_{te})} \tag{3.2}$$

The velocity space resolution is given by $(\Delta v/v_{te}) = 2(v_{max}/v_{te})/n_v$, where n_v is the number of uniformly space points in velocity space between $-v_{max} \leq v \leq +v_{max}$. Thus, our condition becomes

$$\omega_{pe} T_{rec} = \frac{\pi n_v}{k\lambda_{de}(v_{max}/v_{te})} \tag{3.3}$$

To reproduce this effect, we take the case:
$k\lambda_{de} = 0.5$
$\omega_r/\omega_{pe} = 1.43$
$\gamma/\omega_{pe} = -1.59 \times 10^{-1}$

n_x	n_v	v_{max}	n_L	NL	μ	τ	cfl	N_t	n_t out	δn	n_{k1}	$\omega_{pe}T_{rec}$
64	64	5	2	T	100	1	0.5	20000	100	0.1	1	80

The effect of numerical recurrence is demonstrated in Figure 3.5, where the energy as a function of time is plotted both linearly and logarithmically. The clear signature of recurrence at $\omega_{pe}t \sim 80$ is evident in the linear plot. The logarithmic plot shows that the damping rate initially agrees with the prediction from linear theory, but there appears to be a small amplitude recurrence effect at $\omega_{pe}t \sim 40$, with the much stronger numerical recurrence at $\omega_{pe}t \sim 80$.

The lesson here is that, to ensure that even the smaller recurrence effect at $\omega_{pe}t \sim 40$ is avoided, to choose a small enough Δv such that the recurrence time is longer than the simulation time, $T_{rec} > T_{sim}$.

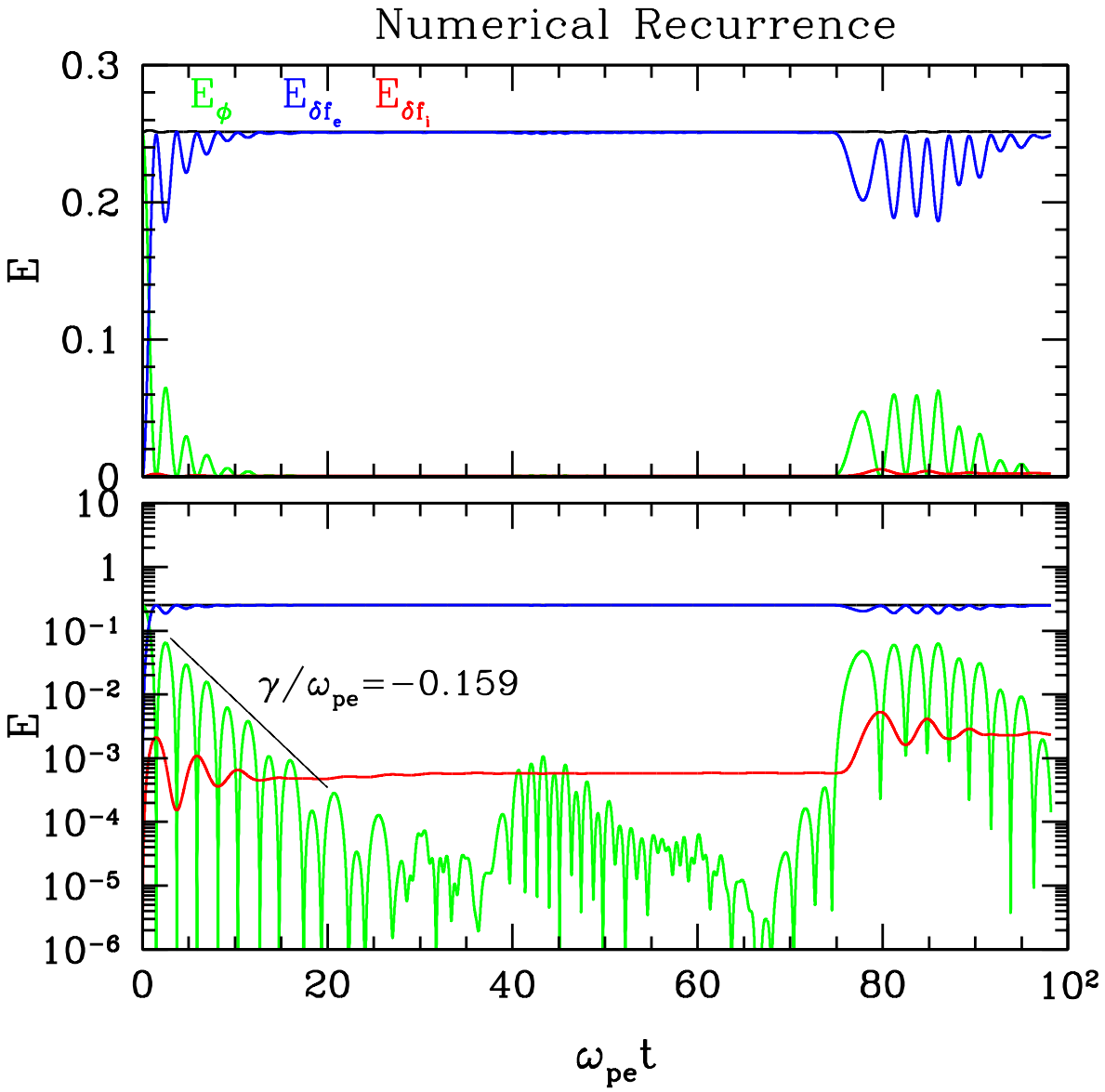

Figure 3.5: Numerical recurrence in a linear run with plasma parameters $\tau = T_i/T_e = 1$ and $\mu = m_i/m_e = 100$. Plotted are the field energy E_ϕ (green), the perturbed electron energy $E_{\delta f_e}$ (blue), the perturbed ion energy $E_{\delta f_i}$ (red), and the total perturbation energy $E_{tot} = E_\phi + E_{\delta f_e} + E_{\delta f_i}$ (black). Numerical recurrence is evident at $\omega_{pe}t \sim 80$.

3.4 Linear Run Comments

1. In linear runs, the δf_{ew} has a constant form (odd in v) and simply decreases in amplitude over time as the electric field damps in amplitude.

2. The initial conditions (any variation of $deltaf$ with x) and the linear wave term $deltaF_{ewl}$ provide the sources for the ballistic term.

3. There is no net energy transfer into the δf_s in the linear runs, because the ballistic term cannot create energy (it just advects energy) and linear wave-particle interaction term both generates a δf_{ew} that is purely odd (and thereby contains no net energy upon integration over v) and because it is also sinusoidal in x (and thereby integrates to zero over the volume).

4. In a linear run, there really is no transfer of energy to the particles. Therefore, the description of energy transfer in collisionless wave-particle interations is inherently incomplete in a linear treatment.

5. *Is the damping of the field then due simply to linear phase mixing?* This should be testable in linear runs to see if the field damping rate obeys linear theory and whether it is due simply to ballistic mixing. I can artificially turn off the linear term and see how fast the field damps in time (due strictly to ballistic term). It may be that the linear wave-particle interactions term feeds the ballistic term in just such a way that you get the right damping rate, and that without that term the field damps (due strictly to linear phase mixing) but at the wrong damping rate.

3.5 Nonlinear Run Comments

1. For weakly damped runs, nonlinear runs effectively have no damping at all. The reason is that, a run is weakly damped (for Langmuir waves, specifically) if the resonant velocity is far out in the tail of the electron distribution function. Thus, it takes very little energy from the wave to flatten that part of the distibution function.

3.6 Final Strategy

In this section I oultine the final strategy to highlight the resonant energy transfer from fields to particles via landau damping, and try to distinguish it from the non-resonant energy transfer that is inherent in linear wave propagation. Normalized and unnormalized correlations of separated parts of the perturbed distribution function, as well as the phase of the maximum correlation, can be used to identify this resonant energy transfer. The resonant aspect, that the signature will occur at the phase velocity, is a key characteristic of Landau damping that I believe is absent for the oscillating energy transfer associated with a wave.

3.6.1 Two Cases: Moderately and Weakly Damped Langmuir Waves

Because the initialization of strictly a uni-directional Langmuir or ion-acoustic wave has proven tricky, I use here just the initialization of a spatial electron density perturbation (`ic=1`) to start the various Landau damping simulations. Note that a purely density perturbation should linear phase mix, whether Landau damping is significnat or not. This can help us to distinguish from the resonant process of Landau damping from the purely kinetic process of linear phase mixing.

Moderately Damped Case

Moderately Damped:
$k\lambda_{de} = 0.5$
$\omega_r/\omega_{pe} = 1.43$
$\gamma/\omega_{pe} = -1.59 \times 10^{-1}$

n_x	n_v	v_{max}	n_L	NL	μ	τ	cfl	N_t	n_t out	δn	n_{k1}
128	256	5	2	T	100	1	0.05	10000	100	0.1	1

Observations:

1. This run appears to yield a good evolution (at least up to $\hat{t} = 49$) without $f_e < 0$ anywhere, and energy conservation is very good.
2. No nonlinear echo behavior up to $t = 49$, although the exponential decay of field energy appears to be arrested around $t = 25$.
3. The ballistic structure develops relatively slowly relative to the timescale of the Landau damping. In this case, the field energy is largely completely gone by $\hat{t} = 18$.
4. The overall odd oscillation in δf_{ew} is due to the wave oscillation behavior, and varies sinusoidally in space. What remains is the quasilinear version of the perturbation when averaged over space.
5. Note, although the δf_{ew} looks even, perhaps the field changes sign and so the signature is heating/damped is thereby the same on both sides?
6. Question: Is a spatial average possible before computing the energy by velocity integration? If so, then the quasilinear pieces of the distribution function tell you about the total change in the distribution function.

7. Note that δf_{ewQL} in Figure 3.8 looks exactly even in v, meaning that the energy transfer will be exactly odd as needed (no need here to separate even and odd!).

Weakly Damped Case

It is important, for weakly damped cases to be properly modeled, that range of velocity space simulated includes the resonant velocity, $v_{max} > \omega/k$. If not, the damping is not properly resolved (in a linear run, the damping rate is too low). Note also that, for weakly damped cases, nonlinear runs effectively have no damping at all. The reason is that a run is weakly damped (for Langmuir waves, specifically) if the resonant velocity is far out in the tail of the electron distribution function. Thus, it takes very little energy from the wave to flatten that part of the distibution function. This is demonstrated in Figure 3.9.

For the weakly damped case, we take the following plasma and numerical parameters:
$k\lambda_{de} = 0.2$
$\omega_r/\omega_{pe} = 1.06$
$\gamma/\omega_{pe} = -4.99 \times 10^{-5}$

n_x	n_v	v_{max}	n_L	NL	μ	τ	cfl	N_t	n_t out	δn	n_{k1}
128	256	8	5	T	100	1	0.25	5000	100	0.025	1

Note that this run becomes numerically unstable at $t > 220$, but this is much longer than we need (it is more than 30 Langmuir wave periods). Reducing `cfl` would delay or cure the computational instability.

This run has effectively no damping of the Langmuir wave, $\gamma = 0$, because wave-particle interactions very easily flatten out the distribution function in the neighborhood of the resonant velocity, as demonstrated in Figure 3.9 below.

New Weakly Damped Case: $k\lambda_{de} = 0.25$

It is important, for weakly damped cases to be properly modeled, that range of velocity space simulated includes the resonant velocity, $v_{max} > \omega/k$. If not, the damping is not properly resolved (in a linear run, the damping rate is too low). Note also that, for weakly damped cases, nonlinear runs effectively have no damping at all. The reason is that a run is weakly damped (for Langmuir waves, specifically) if the resonant velocity is far out in the tail of the electron distribution function. Thus, it takes very little energy from the wave to flatten that part of the distibution function. This is demonstrated in Figure 3.9.

For the weakly damped case, we take the following plasma and numerical parameters:
$k\lambda_{de} = 0.25$
$\omega_r/\omega_{pe} = 1.109$
$\gamma/\omega_{pe} = -2.027 \times 10^{-3}$
$\omega_r/k = 4.436 v_{te}$

n_x	n_v	v_{max}	n_L	NL	μ	τ	cfl	N_t	n_t out	δn	n_{k1}
128	256	6	4	T	100	1	0.05	20000	100	0.025	1

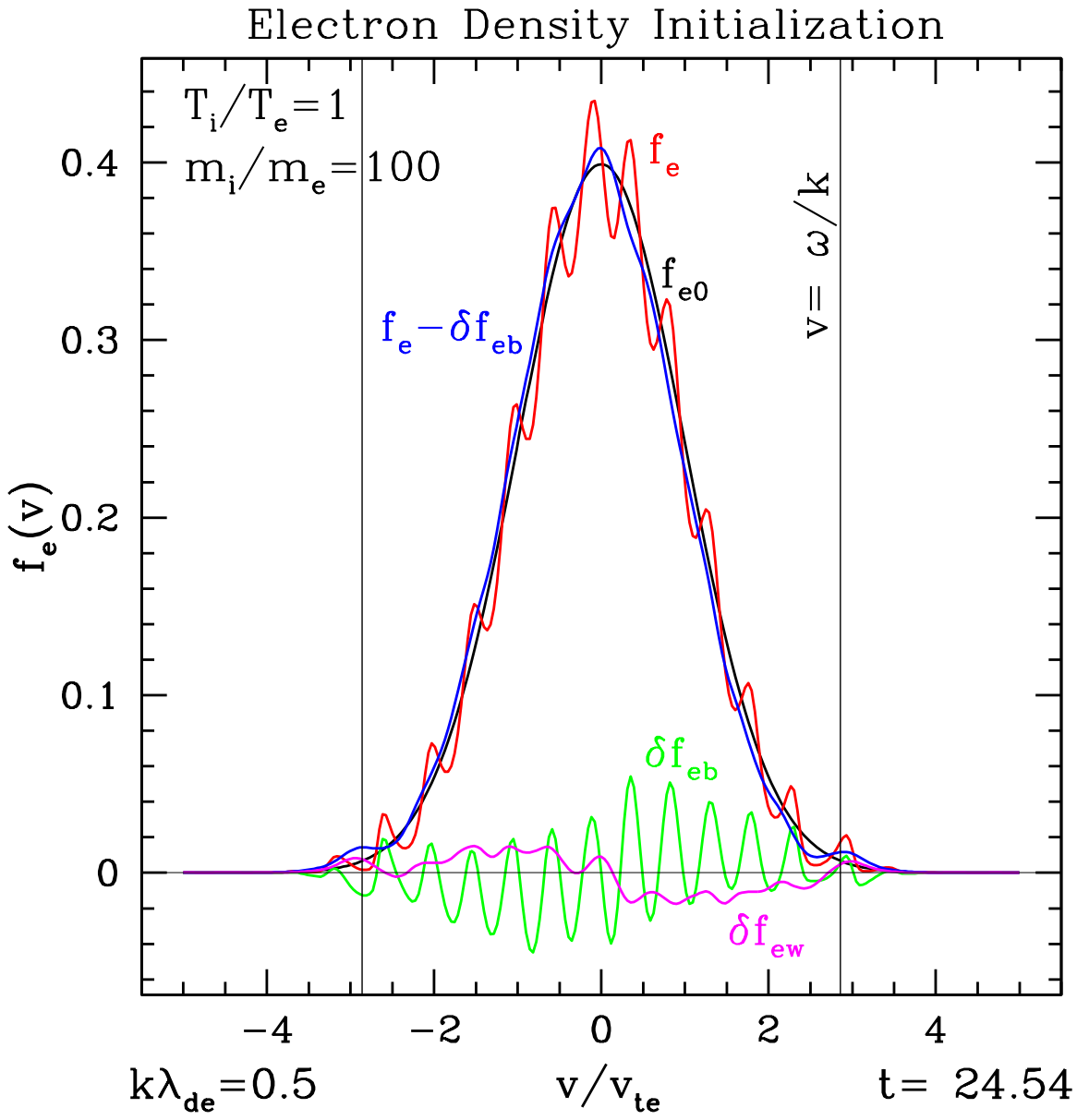

Figure 3.6: The evolution of the electron distribution function due to the Landau damping of a standing Langmuir wave pattern initialized by a sinusoidal electron density perturbation in a plasma with $\tau = T_i/T_e = 1$ and $\mu = m_i/m_e = 100$. Plotted are the equilibrium f_{e0} (black), total f_e (red), ballistic perturbation δf_{eb} (green), wave perturbation δf_{ew} (magenta), and $f_e - \delta f_{eb}$ (blue). Quasilinear flattening is observed at the resonant velocities $v_p/v_{te} = \pm(\omega/\omega_{pe})/(k\lambda de) = \pm 2.83$ (vertical black lines)

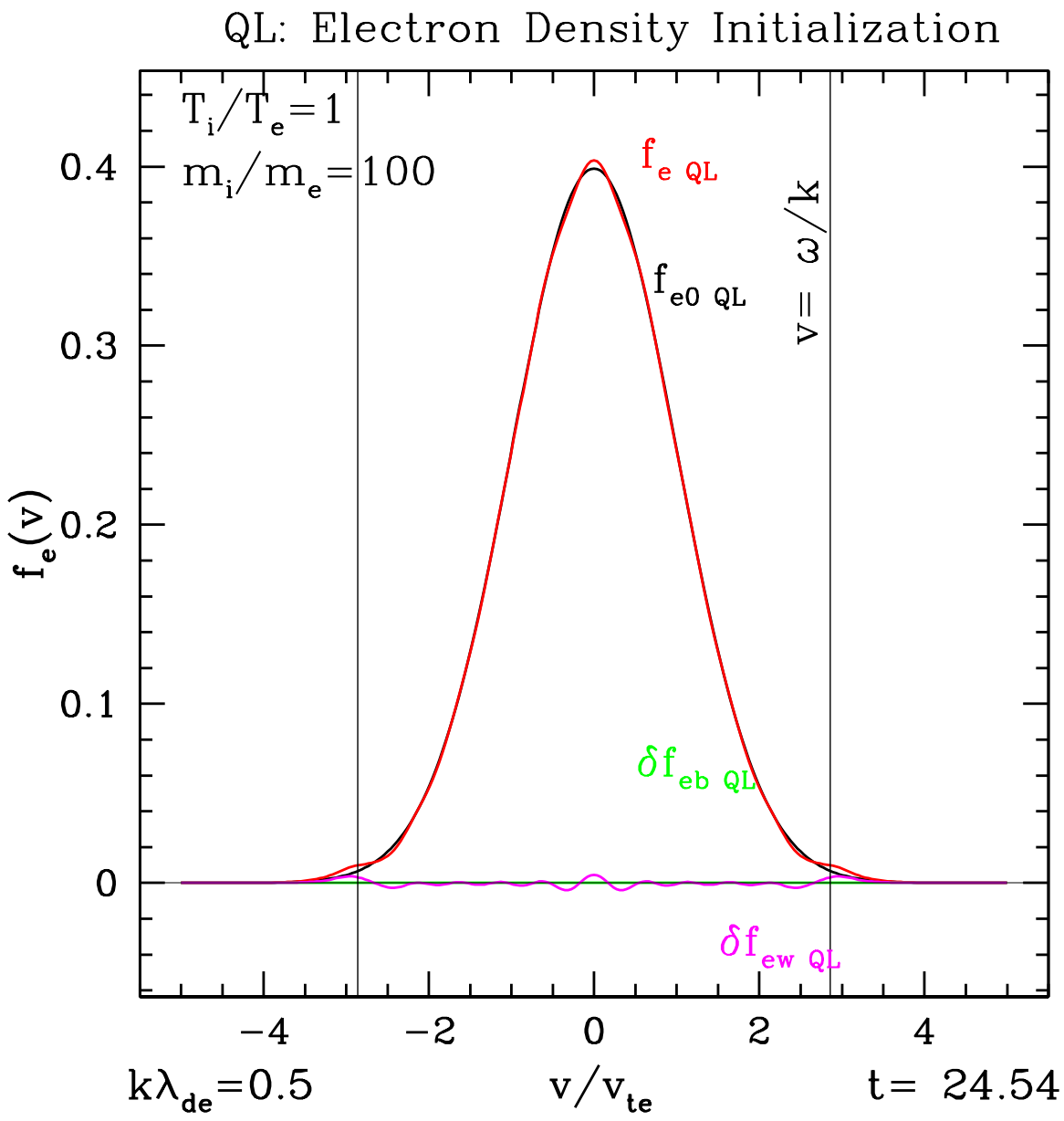

Figure 3.7: The quasilinear evolution of the electron distribution function due to the Landau damping of a standing Langmuir wave pattern initialized by a sinusoidal electron density perturbation in a plasma with $\tau = T_i/T_e = 1$ and $\mu = m_i/m_e = 100$. Plotted are the quasilinear (x-averaged) value for the equilibrium f_{e0QL} (black), total f_{eQL} (red), ballistic perturbation δf_{ebQL} (green), and wave perturbation δf_{ewQL} (magenta). Quasilinear flattening is observed at the resonant velocities $v_p/v_{te} = \pm(\omega/\omega_{pe})/(k\lambda de) = \pm 2.83$ (vertical black lines)

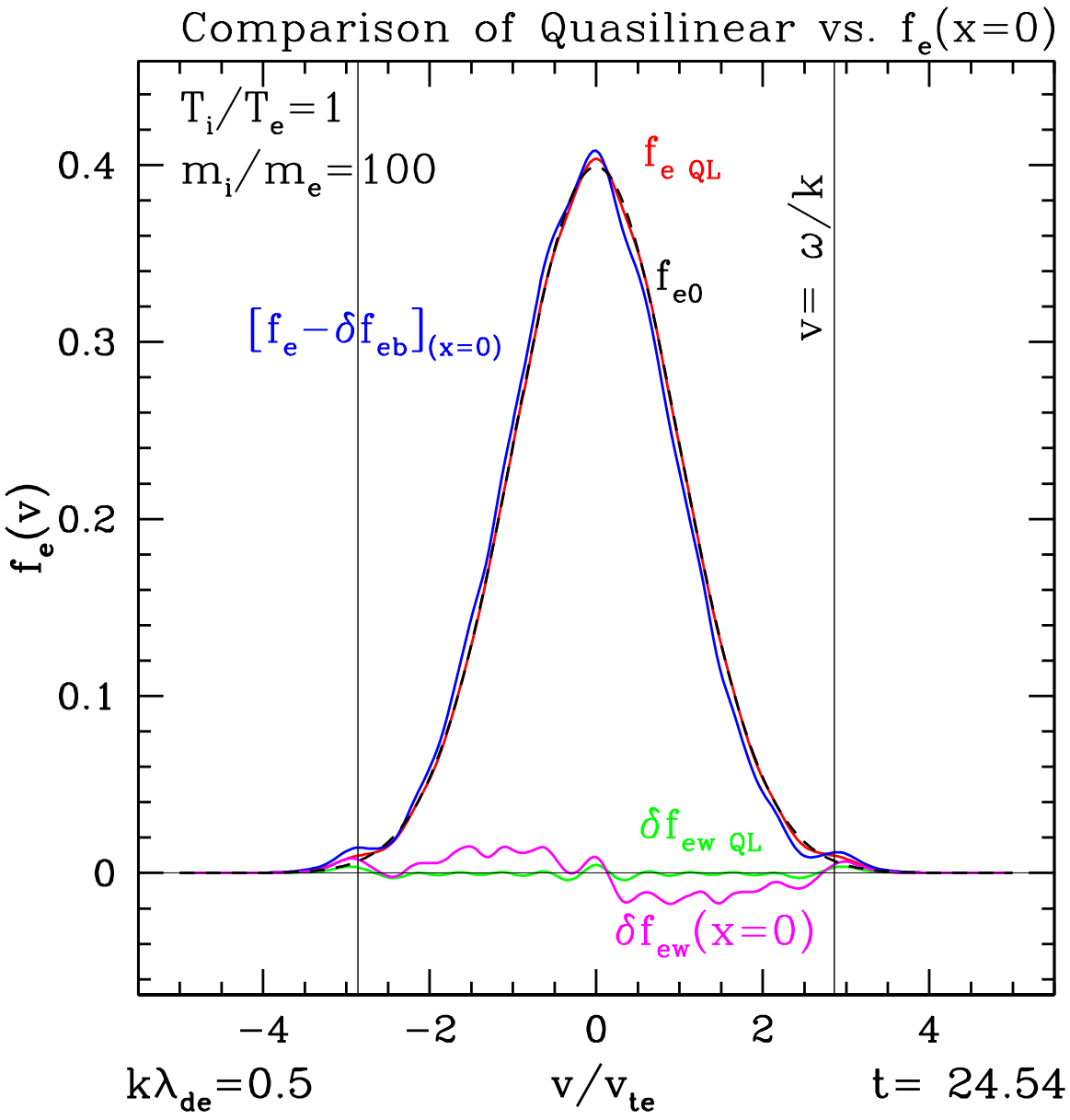

Figure 3.8: Comparison of the quasilinear evolution of the electron distribution function due to the Landau damping of a standing Langmuir wave pattern with the electron distribution function at a particular position in space, $x = 0$. Plasma parameters are $\tau = T_i/T_e = 1$ and $\mu = m_i/m_e = 100$. Plotted are the equilibrium f_{e0} (black), quasilinear f_{eQL} (red), $f_e(x = 0)$ (blue), quasilinear wave perturbation δf_{ewQL} (green), and wave perturbation $\delta f_{ew}(x = 0)$ (magenta). Quasilinear flattening is observed at the resonant velocities $v_p/v_{te} = \pm(\omega/\omega_{pe})/(k\lambda de) = \pm 2.83$ (vertical black lines)

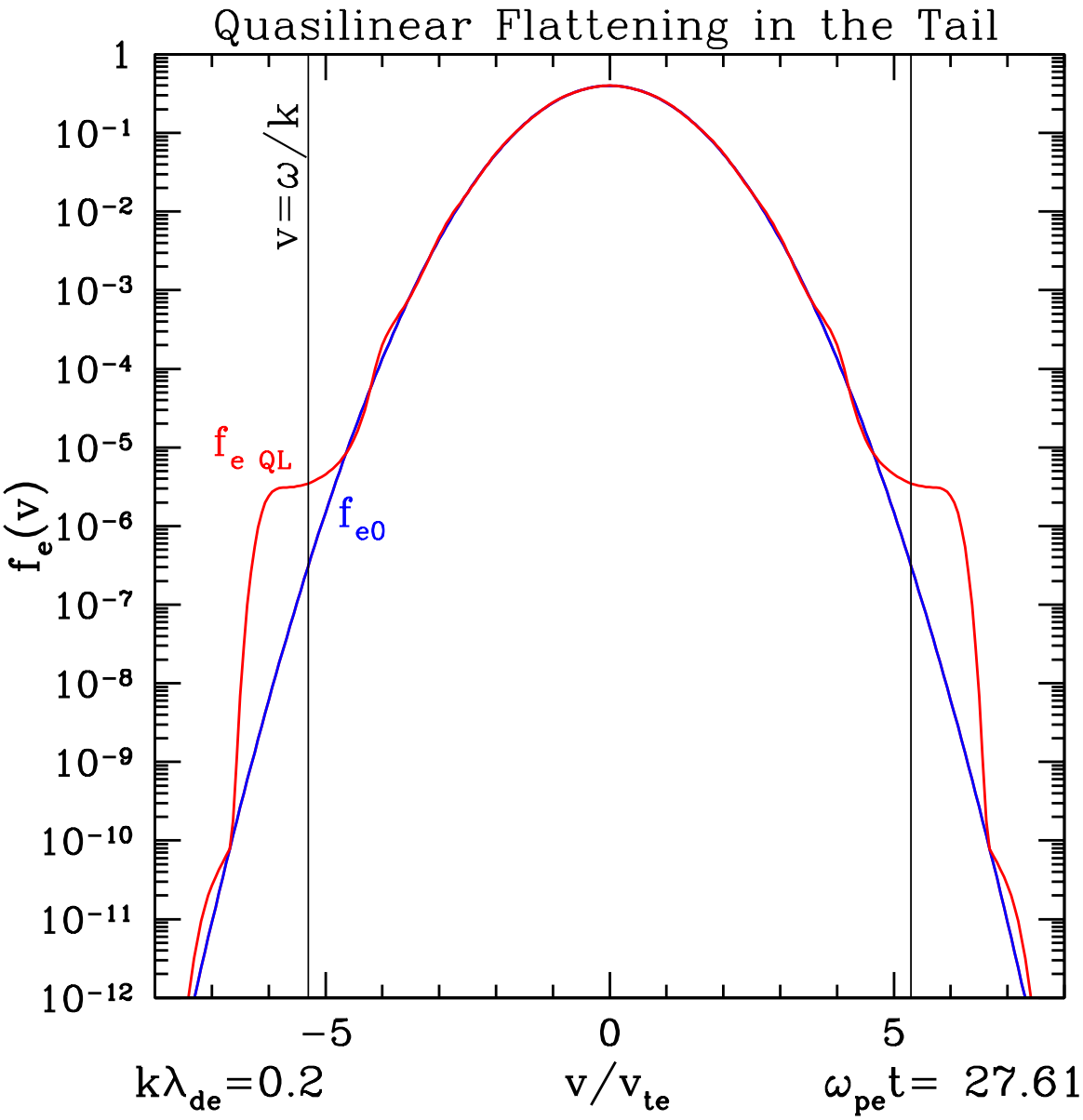

Figure 3.9: For a Langmuir wave simulation (initialized with a spatial electron density perturbation) with plasma parameters $k\lambda_{de} = 0.2$, $\tau = T_i/T_e = 1$, and $\mu = m_i/m_e = 100$. Logarithmically plotted are the equilibrium electron distribution function f_{e0} (blue) and the quasilinear (averaged over x) total electron distribution function f_{eQL} (red) at time $\omega_{pe}t = 27.61$. For a frequency $\omega/\omega_{pe} = 1.06$, the resonant phase velocity is $v/v_{te} = 5.3$, indicated by the vertical black lines.

3.6.2 UPDATED: Theory for Final Strategy

$$\delta f_s = \delta f_{sB} + \delta f_{sWl} + \delta f_{sWn} \tag{3.4}$$

and for notational simplicity I take

$$\delta f_{sW} = \delta f_{sWl} + \delta f_{sWn} \tag{3.5}$$

The time evolution of each component is given by separating the terms of the kinetic equation

$$\frac{\partial \delta f_{sB}}{\partial t} = -v\frac{\partial \delta f_s}{\partial x} \tag{3.6}$$

$$\frac{\partial \delta f_{sWl}}{\partial t} = \frac{q_s}{m_s}\frac{\partial \phi}{\partial x}\frac{\partial f_{s0}}{\partial v} \tag{3.7}$$

$$\frac{\partial \delta f_{sWn}}{\partial t} = \frac{q_s}{m_s}\frac{\partial \phi}{\partial x}\frac{\partial \delta f_s}{\partial v} \tag{3.8}$$

$$\frac{\partial \delta f_s}{\partial t} = -v\frac{\partial \delta f_s}{\partial x} + \frac{q_s}{m_s}\frac{\partial \phi}{\partial x}\frac{\partial f_{s0}}{\partial v} + \frac{q_s}{m_s}\frac{\partial \phi}{\partial x}\frac{\partial \delta f_s}{\partial v}, \tag{3.9}$$

3.6.3 Theory for Final Strategy

I have altered the code of VP to separate out some different terms of the perturbed distribution function. The total decomposition of δf_s now is

$$\delta f_s = \delta f_{sB} + \delta f_{sWl} + \delta f_{sWnb} + \delta f_{sWnw} \tag{3.10}$$

and for notational simplicity I take

$$\delta f_{sW} = \delta f_{sWl} + \delta f_{sWnb} + \delta f_{sWnw}. \tag{3.11}$$

The time evolution of each component is given by separating the terms of the kinetic equation

$$\frac{\partial \delta f_{sB}}{\partial t} = -v\frac{\partial \delta f_{sB}}{\partial x} - v\frac{\partial \delta f_{sW}}{\partial x} \tag{3.12}$$

$$\frac{\partial \delta f_{sWl}}{\partial t} = \frac{q_s}{m_s}\frac{\partial \phi}{\partial x}\frac{\partial f_{s0}}{\partial v} \tag{3.13}$$

$$\frac{\partial \delta f_{sWnb}}{\partial t} = +\frac{q_s}{m_s}\frac{\partial \phi}{\partial x}\frac{\partial \delta f_{sB}}{\partial v} \tag{3.14}$$

$$\frac{\partial \delta f_{sWnw}}{\partial t} = \frac{q_s}{m_s}\frac{\partial \phi}{\partial x}\frac{\partial \delta f_{sW}}{\partial v}. \tag{3.15}$$

Note that it may no be meaningful separate the nonlinear contribution to the evolution into a nonlinear ballistic (nb) and nonlinear wave (nw) part. In fact, a few initial tests of the weakly damped case show that the energy associated with δf_{eWnb} becomes negative at times, whereas really only the combined nonlinear component δf_{sWn} seems to be physically required to be positive. (In fact, all this separation is rather artificial, and really only the sum of all pieces must be nonnegative, $f_s > 1$.) If it turns out that the separation of δf_{eWnb} and δf_{sWnw} is not meaningful, I may remove it from

the code (because it does slow down the code). However, if there is any simplification, this separation may yield further insight.

Energetic arguments help us to identify which components of the perturbed distribution function are associated with the change in the energy of the particles (due to Landau damping). Although a general case (spacecraft measurements or nonlinear gyrokinetic simulations) cannot separate out the different constributions $\delta f_s = \delta f_{sB} + \delta f_{sWl} + \delta f_{sWnb} + \delta f_{sWnw}$, we hope to identify of strategy of correlation measurements that can highlight this signature *without* the separation of these different contributions to δf_s. Here I outline the simple arguments about energy conservation (some repitition from the Theory section).

The *conserved Vlasov-Poisson energy* is given by

$$W = \int d^3\mathbf{x} \frac{|\mathbf{E}|^2}{8\pi} + \sum_s \int d^3\mathbf{x} \int dv \frac{1}{2} m_s v^2 f_s. \tag{3.16}$$

Taking the time derivative of this conserved energy, we find that the energy gain by the particles must be equal to the energy lost from the electrostatic field,

$$\frac{\partial}{\partial t} \sum_s \int d^3\mathbf{x} \int dv \frac{1}{2} m_s v^2 f_s = -\frac{\partial W_\phi}{\partial t} \tag{3.17}$$

Therefore, the rate of energy exchange (gain or loss) for a species s is given by

$$\frac{\partial W_s}{\partial t} = \frac{\partial}{\partial t} \int d^3\mathbf{x} \int dv \frac{1}{2} m_s v^2 f_s = \int d^3\mathbf{x} \int dv \frac{1}{2} m_s v^2 \frac{\partial f_s}{\partial t} \tag{3.18}$$

We focus here on the energy gain by species s, with the assumption that the total distribution function is given by

$$f_s(x, v, t) = f_{s0}(v) + \delta f_s(x, v, t), \tag{3.19}$$

where the equilibirum distribution function is assumed to be uniform in space and static in time. We also make the additional assumption that $f_{s0}(v)$ is an *even function of velocity*, but it need not be a Maxwellian.

By substituting into (3.18) for $\frac{\partial f_s}{\partial t}$ from the kinetic equation with the different contributions of the perturbed distribution function in (3.10) separated out, we obtain

$$\frac{\partial W_s}{\partial t} = \int d^3\mathbf{x} \int dv \frac{1}{2} m_s v^2 \frac{\partial f_s}{\partial t} = \int d^3\mathbf{x} \int dv \frac{1}{2} m_s v^2 \left[-v \frac{\partial \delta f_s}{\partial x} + \frac{q_s}{m_s} \frac{\partial \phi}{\partial x} \frac{\partial f_{s0}}{\partial v} + \frac{q_s}{m_s} \frac{\partial \phi}{\partial x} \frac{\partial \delta f_{sB}}{\partial v} + \frac{q_s}{m_s} \frac{\partial \phi}{\partial x} \frac{\partial \delta f_{sW}}{\partial v} \right] \tag{3.20}$$

In this equation, only the last two terms contribute to a non-zero change in the particle energy (after integrating over velocity space and space).

The first term, the ballistic term, can expressed as a perfect differential in x,

$$\int dx \int dv \frac{1}{2} m_s v^2 \left[-v \frac{\partial \delta f_s}{\partial x} \right] = \int dx \frac{\partial}{\partial x} \left[\int dv \frac{1}{2} m_s v^2 \delta f_s \right] = 0 \tag{3.21}$$

so for periodic or infinite boundaries yields a zero value.

The second term may be written

$$\int dx \int dv \frac{1}{2} m_s v^2 \left[\frac{q_s}{m_s} \frac{\partial \phi}{\partial x} \frac{\partial f_{s0}}{\partial v} \right] = \int dx \frac{q_s}{2} \frac{\partial \phi}{\partial x} \left[\int dv \;\; v^2 \frac{\partial f_{s0}}{\partial v} \right] = \int dx \frac{\partial}{\partial x} \left\{ \frac{q_s \phi}{2} \left[\int dv \;\; v^2 \frac{\partial f_{s0}}{\partial v} \right] \right\} = 0. \tag{3.22}$$

Since we have chosen f_{s0} to be an even function of v, then its derivative $\partial f_{s0}/\partial v$ is an odd function, so the integrand of the velocity integral becomes an odd function evaluated over an even interval, yielding zero. Another way to see this is to replace evaluate the derivative as $\partial f_{s0}/\partial v = -(v/v_{ts}^2) f_{s0}$, leading to a velocity integral

$$- \int_{-\infty}^{\infty} dv \frac{v^3}{v_{ts}^2} f_{s0} = 0. \tag{3.23}$$

since, with f_{s0} even, the integrand is once again odd. In addition, because f_{s0} is not a function of x, everything in the curly braces is also a perfect differential, so this term also vanishes over integration over all space.

This leaves the last two terms as the only ones possibly responsible for the resonant energy transfer in Landau damping. Note that, we can also separate the energy associated with these two components (not taking the time derivative of W_s), to yield

$$W_s = \frac{\partial}{\partial t} \sum_s \int d^3\mathbf{x} \int dv \frac{1}{2} m_s v^2 (\delta f_{sWnb} + \delta f_{sWnw}) \tag{3.24}$$

Since the velocity integral is nonzero only for the even components of δf_{sWnb} and δf_{sWnw}, visual inspection of these components can help us see the signature of Landau damping in velocity space. Note, however, that I do not think we should actually take just the even component—our diagnostics should be able to distinguish this without separating odd and even components.

3.6.4 Results for Weakly Damped Case

First, we plot the different components of the perturbed electron distribution function for the weakly damped case. Plotted in Figure 3.11 are the components of the perturbed electron distribution function. Note that the two components that lead to a secular transfer of energy, δf_{sWnb} (red) and δf_{sWnw}, are the smallest contributions. Thus, it will be necessary to separate this smaller signal from the larger signals.

Next, we plot the quasilinear (x-averaged) distribution function components at the same time with sufficient zoom to see that structure at the resonant phase velocity. Note that, in this plot, you can see in the δf_{sWnb} component (red) the resonant signature of flattening of the distribution function. In this weakly damped case, there is very little energy transfer, but nonetheless this is the signature of the quasilinear evolution due to Landau damping way out in the tail of the distribution function.

What we want to do is perform correlations of the electric field with the different components δf_{sj} of the distributin function (where j stands for any of the different components), $C(E, q_s v \delta f_{sj})$. Looking at both the normalized and unnormalized correlation, as well as the phase of the maximum correlation, will hopefully enable us to see that resonant effect (even in this very weakly damped case, which is probably unobservable in nonlinear GK simulations and spacecraft measurements). Note, we should do correlations with the following δf_{sj}:

1. δf_{sB}

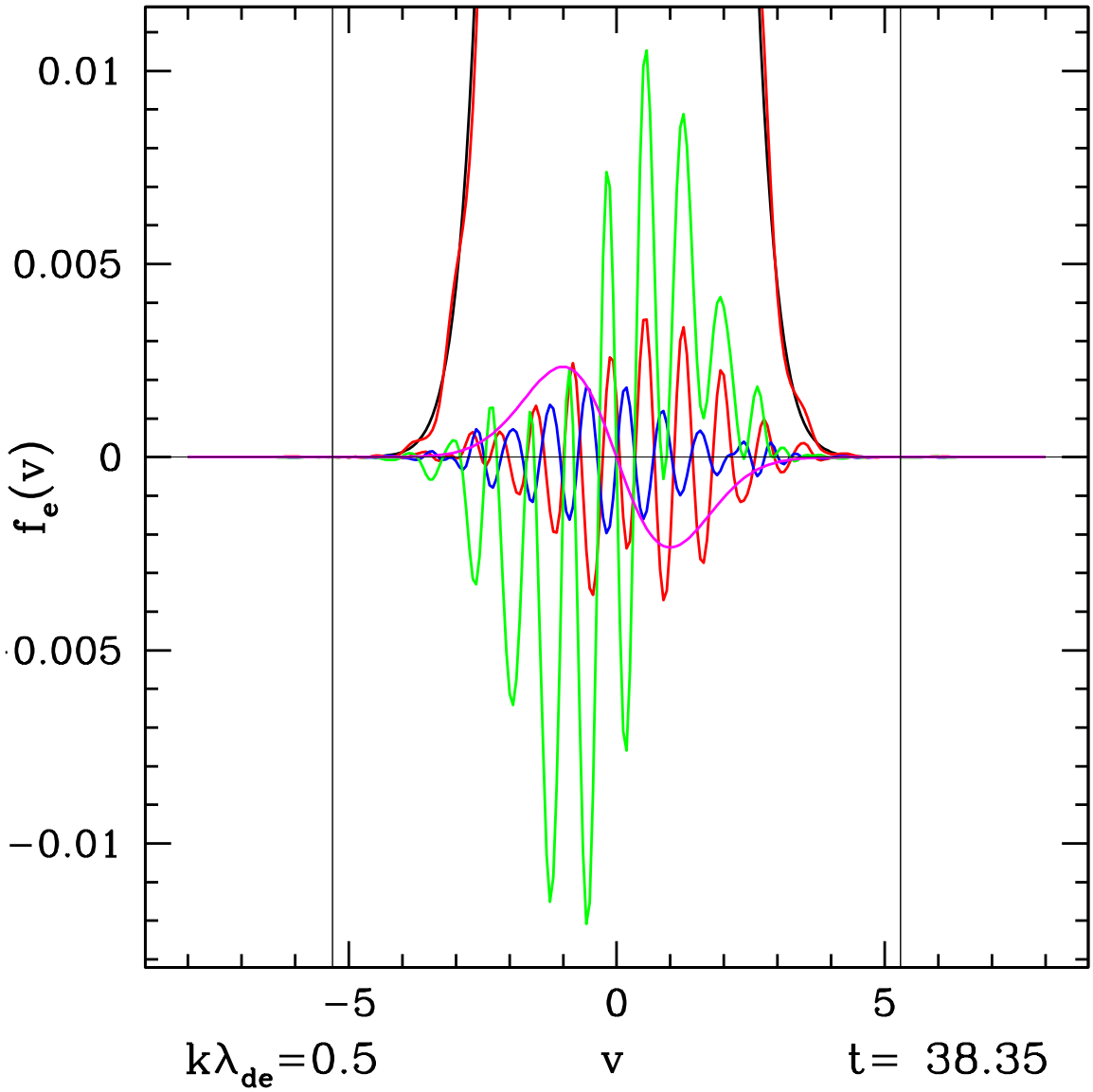

Figure 3.10: Perturbed electron distribution function components: (a) δf_{sB} (green), (b) δf_{sWl} (magenta), (c) δf_{sWnb} (red) ,and (d) δf_{sWnw} (blue). Also plotted are the equilibirum electron distribution function f_{e0} (black) and the total electron distribution function f_e (red). Vertical black bars are the resonant velocity. (NOTE $k\lambda_{de} = 0.2$ is labelled wrong on plot.)

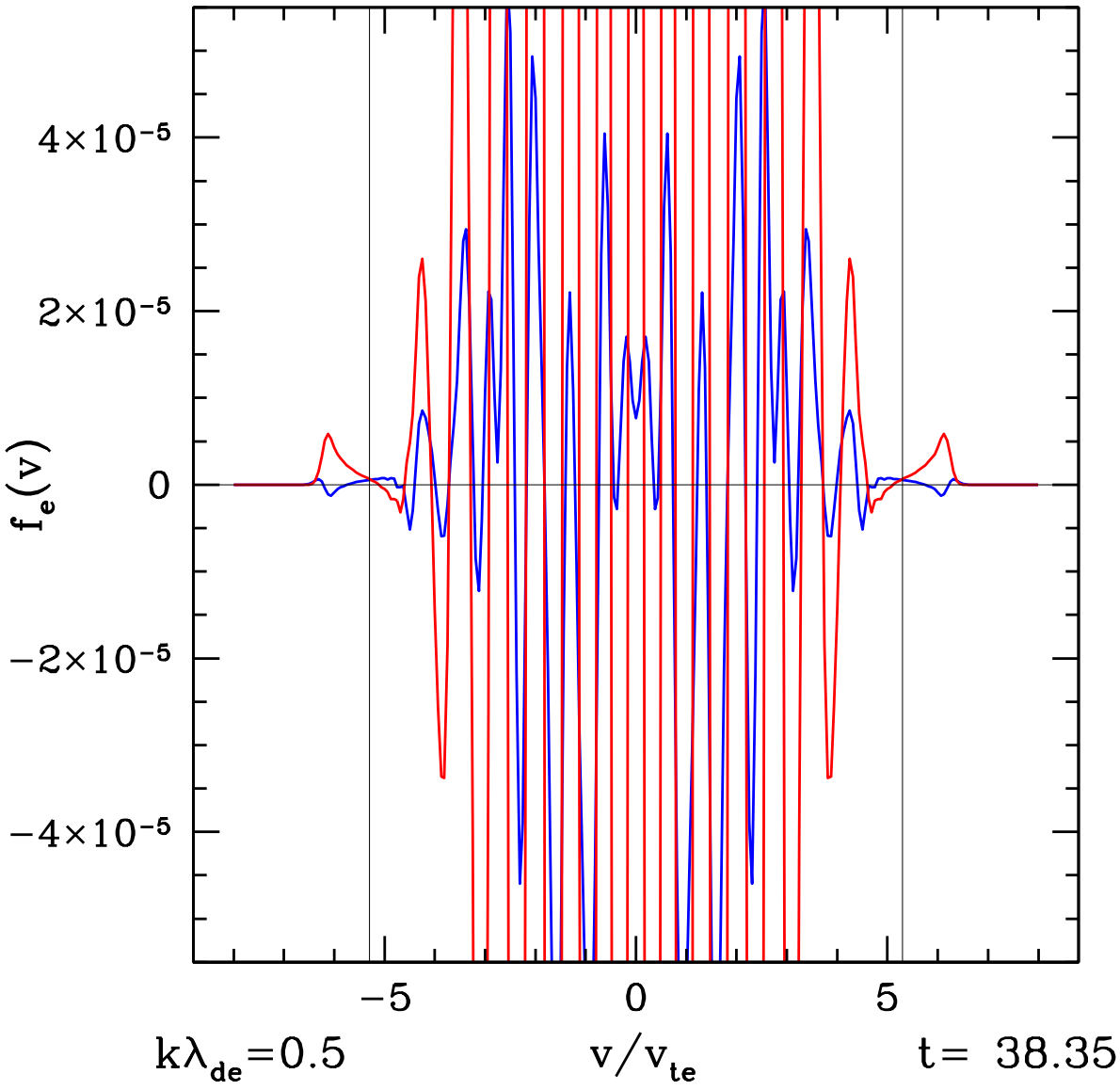

Figure 3.11: Quasilinear (x-averaged) perturbed electron distribution function components: (a) δf_{sWnb} (red) and (b) δf_{sWnw} (blue). Vertical black bars are the resonant velocity. (NOTE $k\lambda_{de} = 0.2$ is labelled wrong on plot.)

2. δf_{sWl} This is the wave part of the energy transfer.

3. δf_{sWnb}

4. δf_{sWnw}

5. $\delta f_{ewn} = \delta f_{sWnb} + \delta f_{sWnw}$ Note that this one is important, because the separation of these two components may not be meaningful.

3.6.5 Results for Moderately Damped Case

The energy evolution of the plasma is best examined looking at the total perturbed energy (no including the equilibrium ion and electron energy), $W_{\delta tot} = W_\phi + W_{\delta f_e} + W_{\delta f_i}$, as plotted in Figure 3.12. The perturbed electron energy is further split into its components: the linear wave $W_{\delta f_e Wl}$ (not plotted), nonlinear ballistic $W_{\delta f_e Wnb}$ (blue dashed) and nonlinear wave $W_{\delta f_e Wnw}$ (blue dotted) contributions. Note that the linear wave component $W_{\delta f_e Wl}$ has zero energy, as expected theoretically, as does the (linear) ballistic energy associated with δf_{eB}.

Looking at the perturbed electron distribution function in Figure 3.11, we note that the nonlinear wave contributions are again very small (blue and red) relative to the linear wave (magenta) and linear ballistic (green) contributions. Note in particular that the nonlinear ballistic δf_{sWnb} (red) part seems to have some structure associated with the resonant velocity (vertical black lines). On the other hand, the nonlinear wave δf_{sWnw} (blue) seems to have very little magnitude at the resonant velocity. (Of course, their sum $\delta f_{ewn} = \delta f_{sWnb} + \delta f_{sWnw}$ would still have the structure at the resonant velocity.)

Next, we can look at the the quasilinear (x-averaged) distribution function components to see the structure at the resonant phase velocity. In Figure 3.14, we plot the contributions δf_{sWnb} (red) δf_{sWnw} (blue) as well as the total (x-averaged) quasilinear distribution function f_{eQL} (red). Here you can see that the δf_{sWnb} component seems to dominate the quasilinear flattening observed at the resonant velocity. In Figure 3.15, we plot a zoomed version of δf_{sWnb} (red) and δf_{sWnw} (blue). Note that both of these functions appear to be dominantly even, meaning they will contribute non-negligibly when multiplied by v^2 and integrated over velocity to get energy.

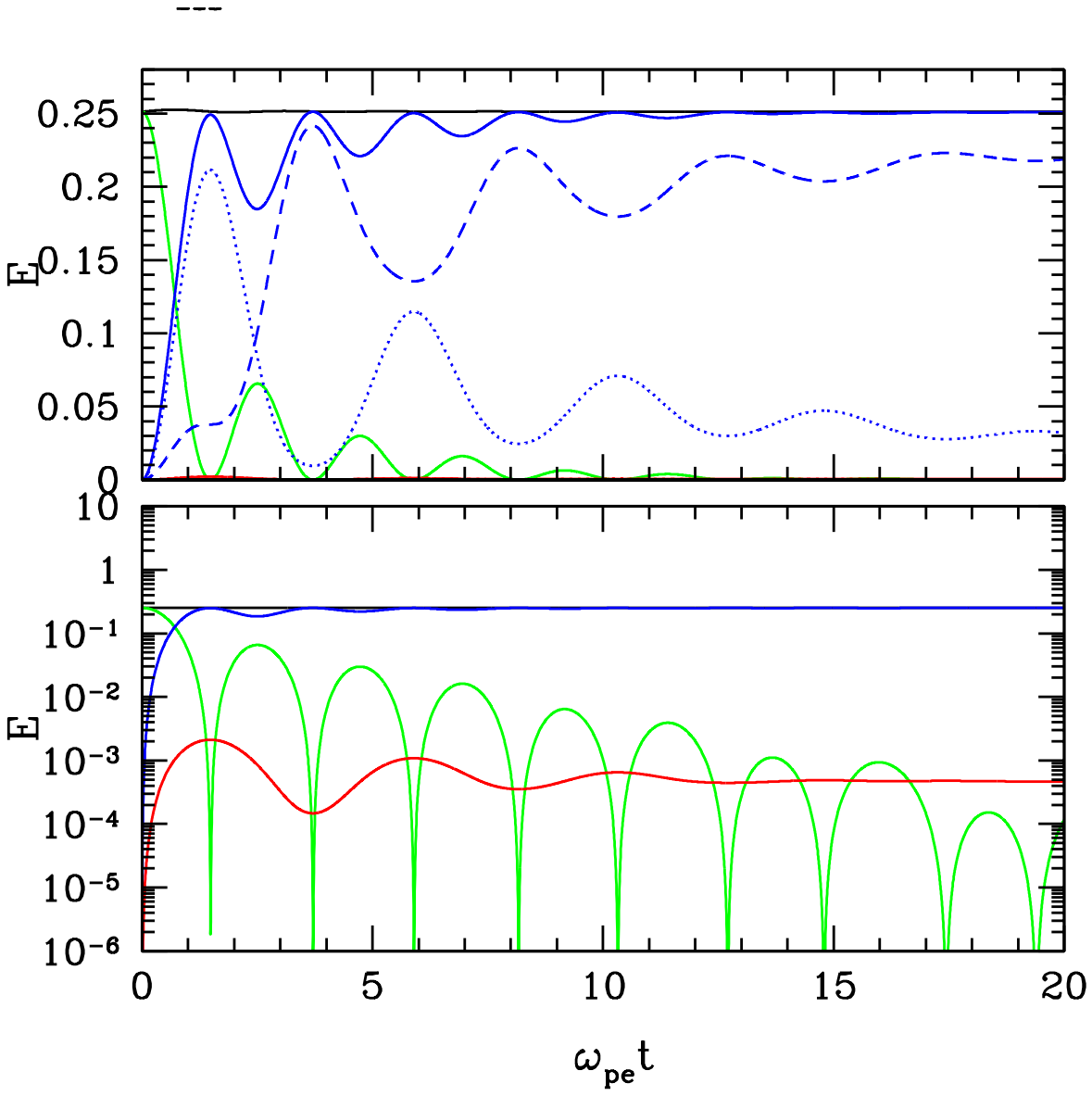

Figure 3.12: Energy evolution for the moderately damped case up to $\omega_{pe}t = 20$. Plotted are the total perturbed energy $W_{\delta tot}$ (black), field energy W_{ϕ} (green), perturbed ion energy $W_{\delta f_i}$ (red), and perturbed electron energy $W_{\delta f_e}$ (blue). The perturbed electron energy is further split into the nonlinear ballistic $W_{\delta f_e Wnb}$ (blue dashed) and nonlinear wave $W_{\delta f_e Wnw}$ (blue dotted) contributions.

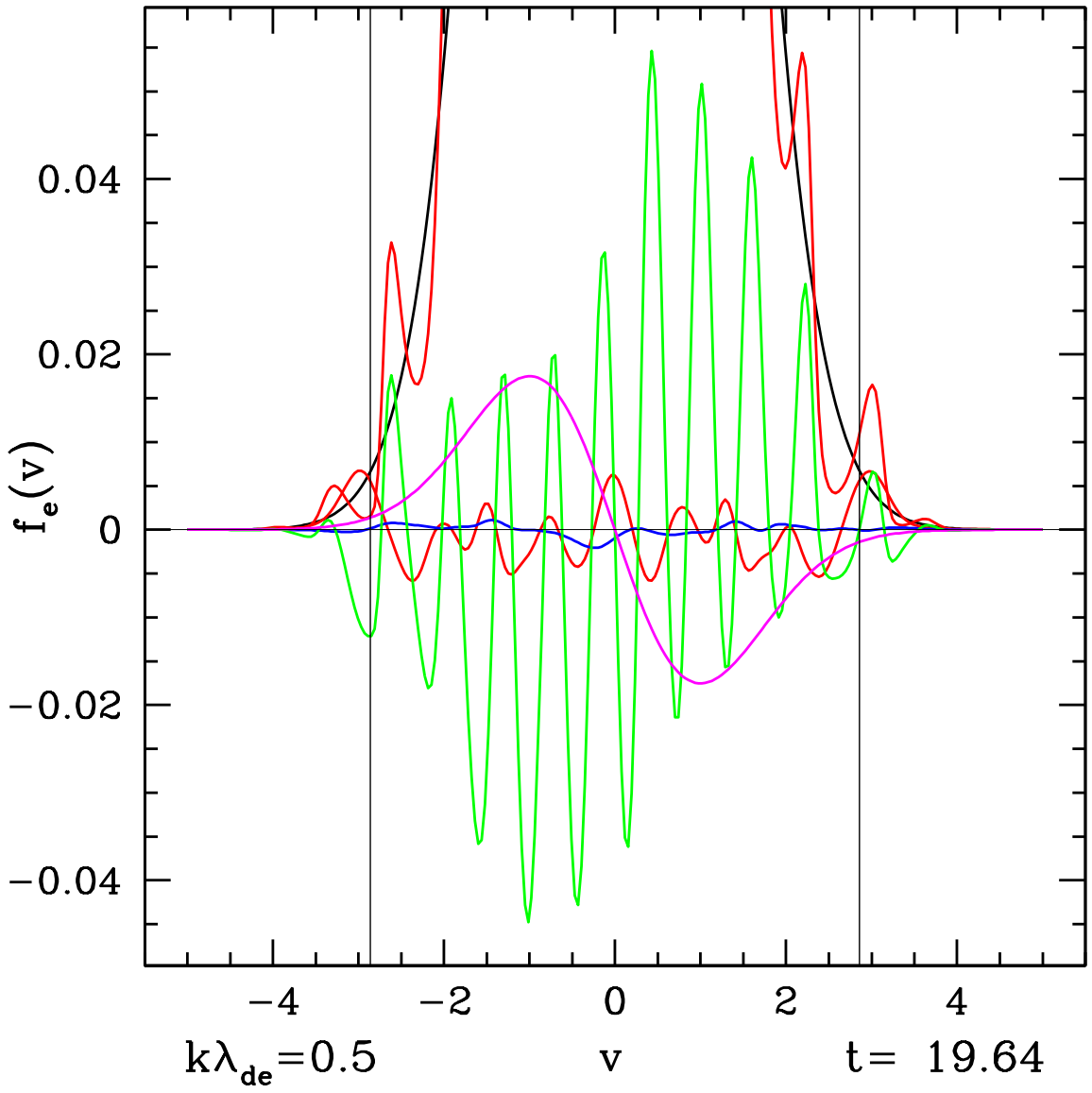

Figure 3.13: Perturbed electron distribution function components: (a) δf_{sB} (green), (b) δf_{sWl} (magenta), (c) δf_{sWnb} (red) ,and (d) δf_{sWnw} (blue). Also plotted are the equilibirum electron distribution function f_{e0} (black) and the total electron distribution function f_e (red). Vertical black bars are the resonant velocity.

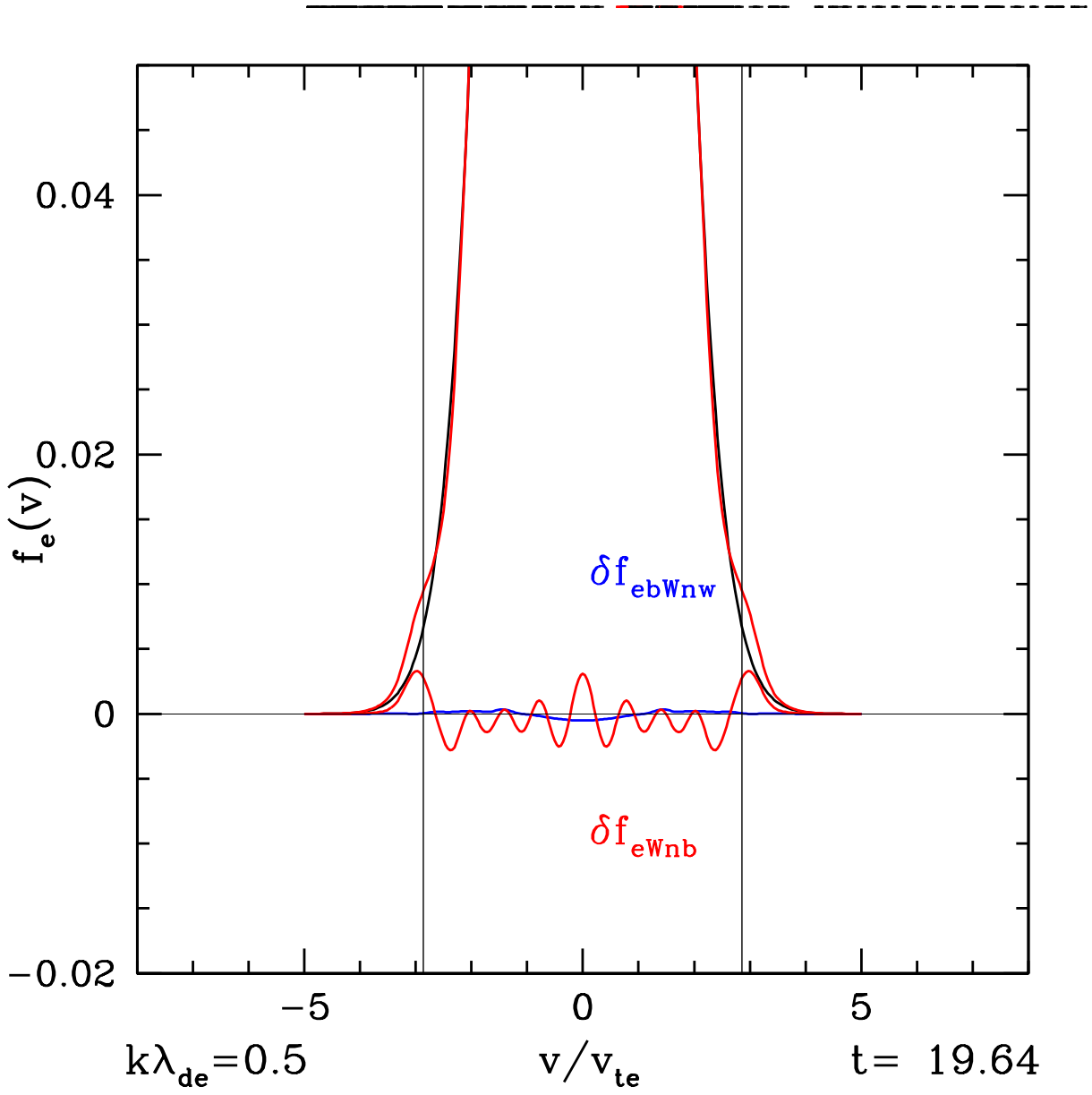

Figure 3.14: Quasilinear (x-averaged) perturbed electron distribution function components: (a) f_{e0} (black), (b) f_{eQL} (red), (c) δf_{sWnb} (red), and (d) δf_{sWnw} (blue). Vertical black bars are the resonant velocity.

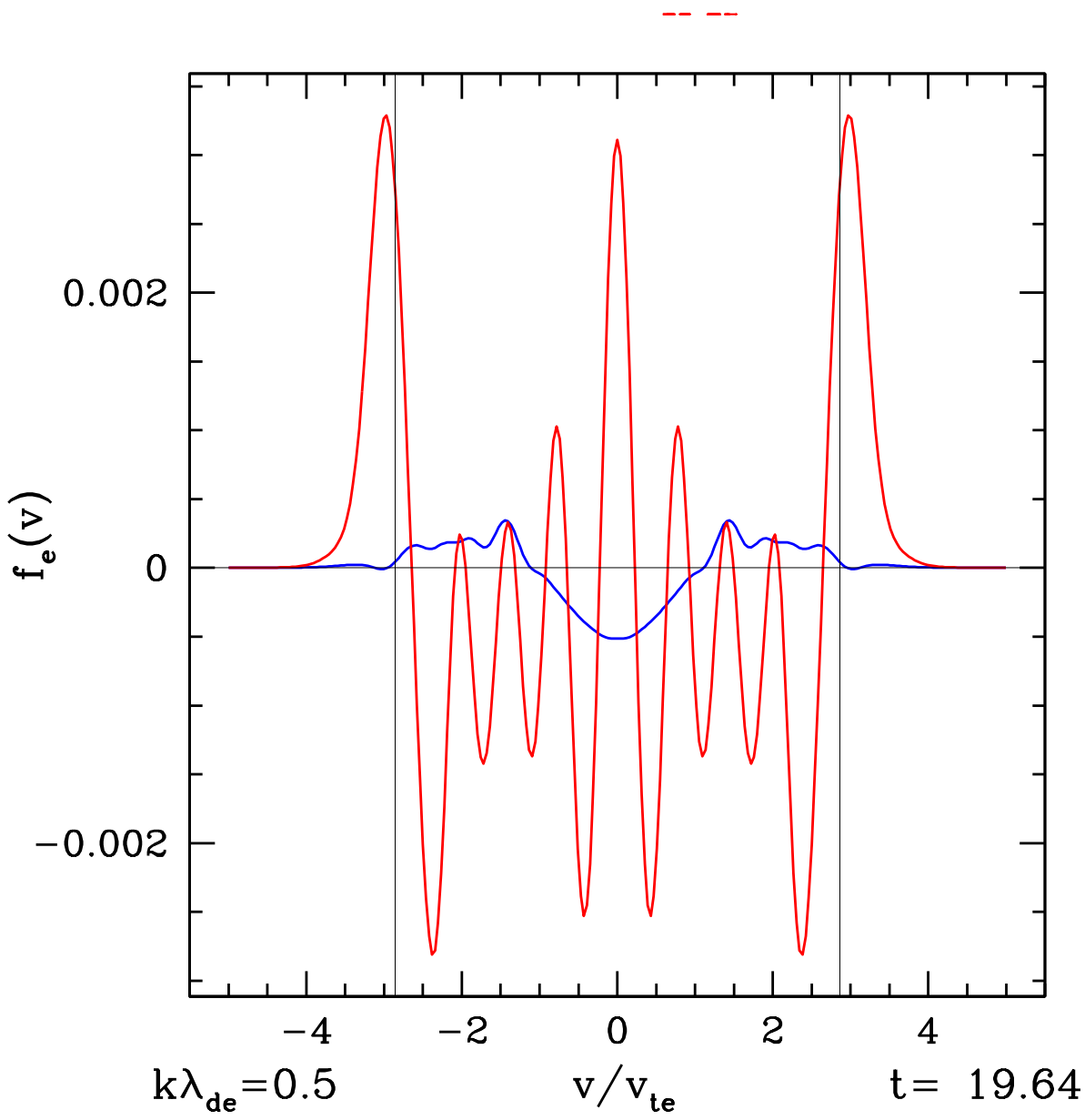

Figure 3.15: Quasilinear (x-averaged) perturbed electron distribution function components: (a) δf_{sWnb} (red) and (b) δf_{sWnw} (blue). Vertical black bars are the resonant velocity.

3.6.6 Work to do with Correlations

What we want to do is perform correlations of the electric field with the different components δf_{sj} of the distributin function (where j stands for any of the different components), $C(E, q_s v \delta f_{sj})$. Looking at both the normalized and unnormalized correlation, as well as the phase of the maximum correlation, will hopefully enable us to see that resonant effect (even in this very weakly damped case, which is probably unobservable in nonlinear GK simulations and spacecraft measurements). Note, we should do correlations with the following δf_{sj}:

1. δf_{sB}
2. δf_{sWl} This is the wave part of the energy transfer.
3. δf_{sWnb}
4. δf_{sWnw}
5. $\delta f_{ewn} = \delta f_{sWnb} + \delta f_{sWnw}$ Note that this one is important, because the separation of these two components may not be meaningful.

Note that the results above suggest that the correlation of $C(E, q_s v \delta f_{eWnb})$ should produce a significant signature at the resonant velocity for the moderately damped case. The normalized signature should be a shift from positive to negative correlation at $v = \omega/k$, and the unnormalized signature should have a peak in the amplitude of the product of these two tersm around this resonant velocity. There may also be a difference in the the correlated phase (with electric field) of the linear wave component δf_{sWl} relative to the nonlinear wave ballistic component δf_{sWnb} (or the sum of the nonlinear components, $\delta f_{ewn} = \delta f_{sWnb} + \delta f_{sWnw}$).

3.7 Line Plots of Contributions to $\delta w_s(x_0, v, t)/\delta t$

The rate of change of phase-space energy density is given by

$$\frac{\partial W_s}{\partial t} = -\int dx \int dv \; q_s \frac{v^2}{2} \frac{\partial \delta f_s(x,v,t)}{\partial v} E(x,t) = \int dx \int dv \; q_s v \delta f_s(x,v,t) E(x,t), \tag{3.25}$$

where we focus on the first form of the equation. Since we have decomposed $\delta f_s(x,v,t)$ into $\delta f_e = \delta f_{eB} + \delta f_{eWl} + \delta f_{eWn}$, it is interesting to ask the question: *Which these sub-components is responsible for the rate of change of phase-space energy density?*

Note also that only the even component of this term survives when intergrated over velocity, so looking at just the even component will help to isolate the signal that is responsible for the resonant energy transfer.

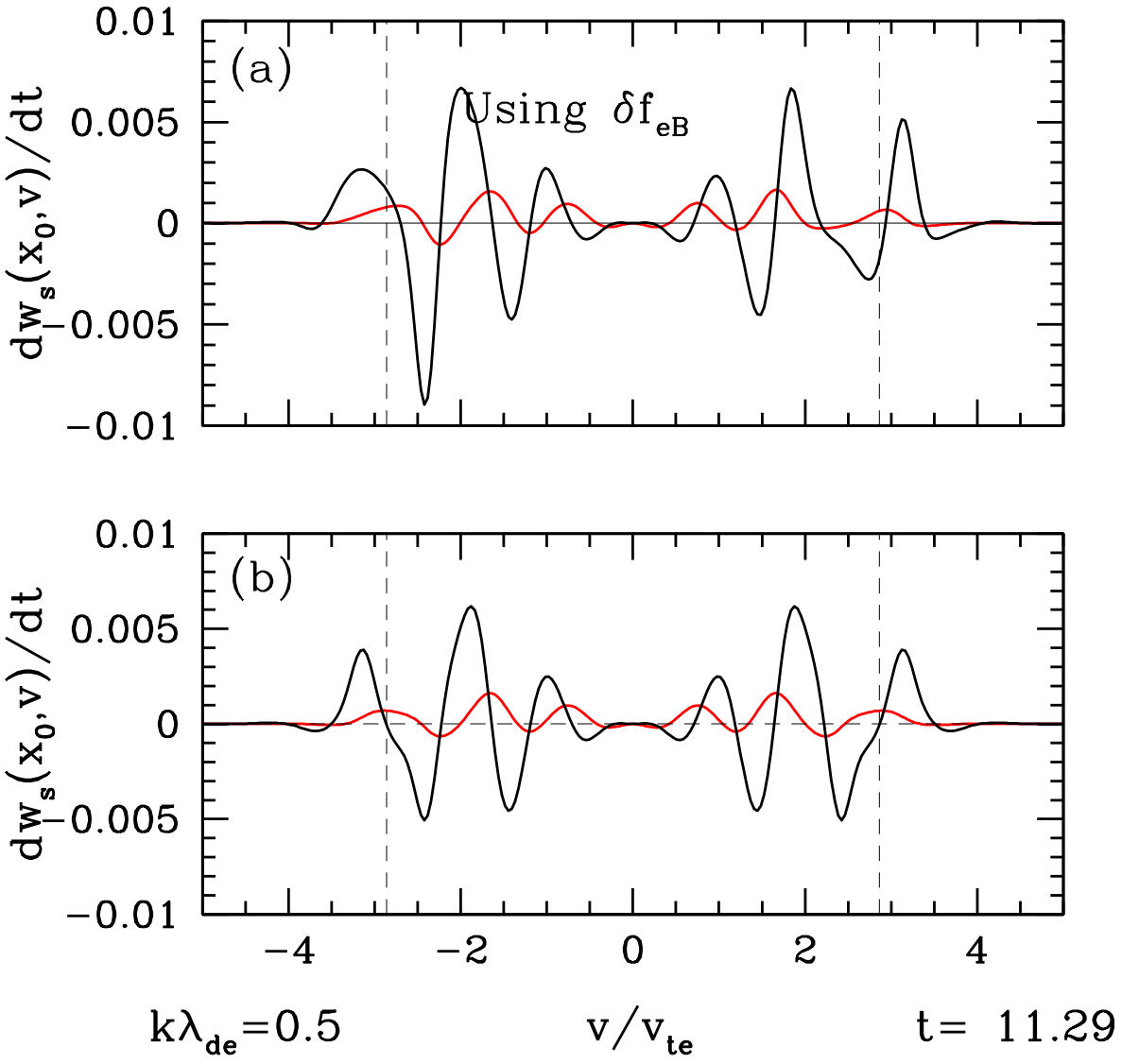

Figure 3.16: Plot of the (a) complete and (b) just even (in v) component of $q_e \frac{v^2}{2} \frac{\partial \delta f_{eB}(x,v,t)}{\partial v} E(x_0,t)$ at $x_0 = 0$.

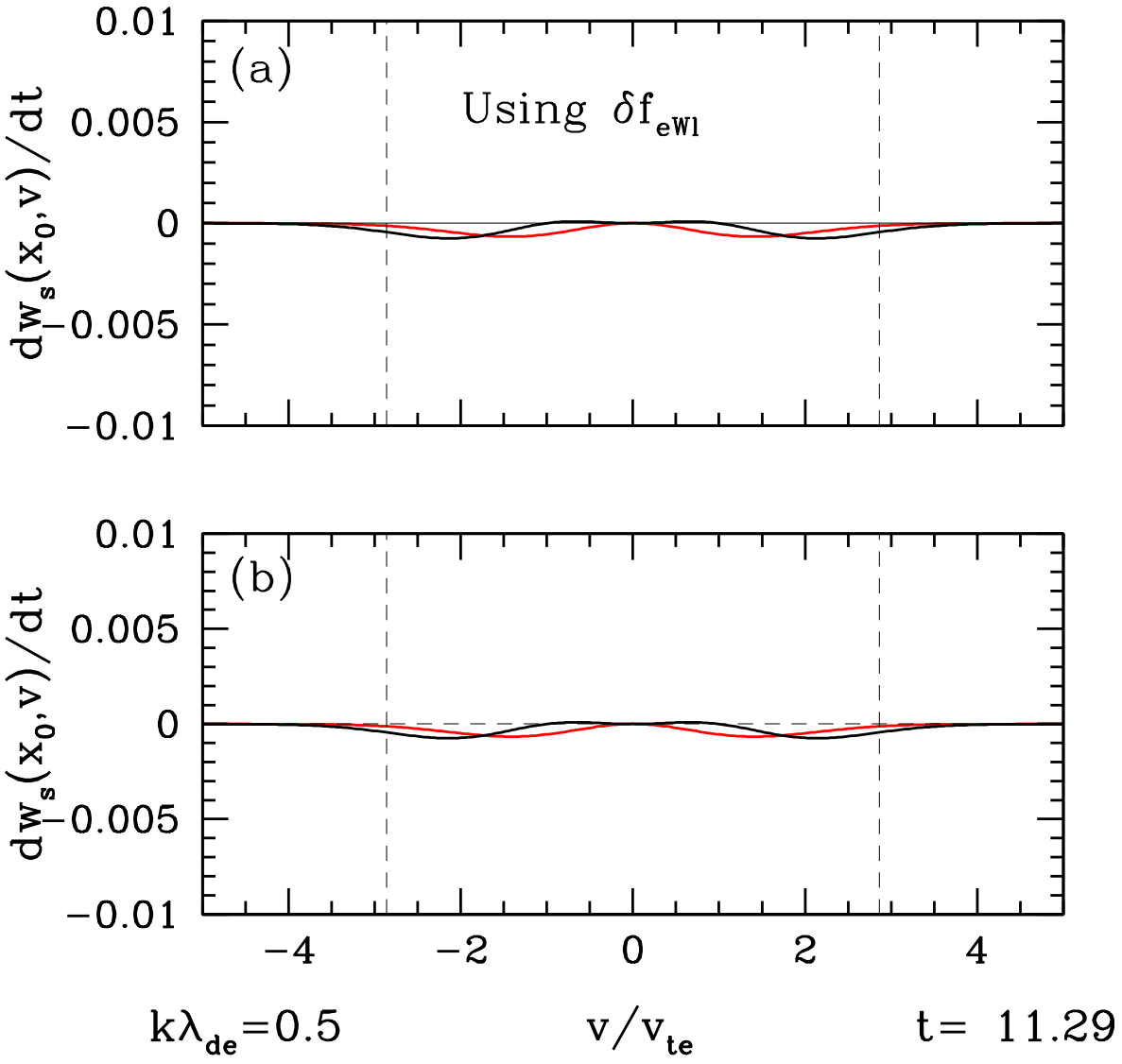

Figure 3.17: Plot of the (a) complete and (b) just even (in v) component of $q_e \frac{v^2}{2} \frac{\partial \delta f_{eWl}(x,v,t)}{\partial v} E(x_0,t)$ at $x_0 = 0$.

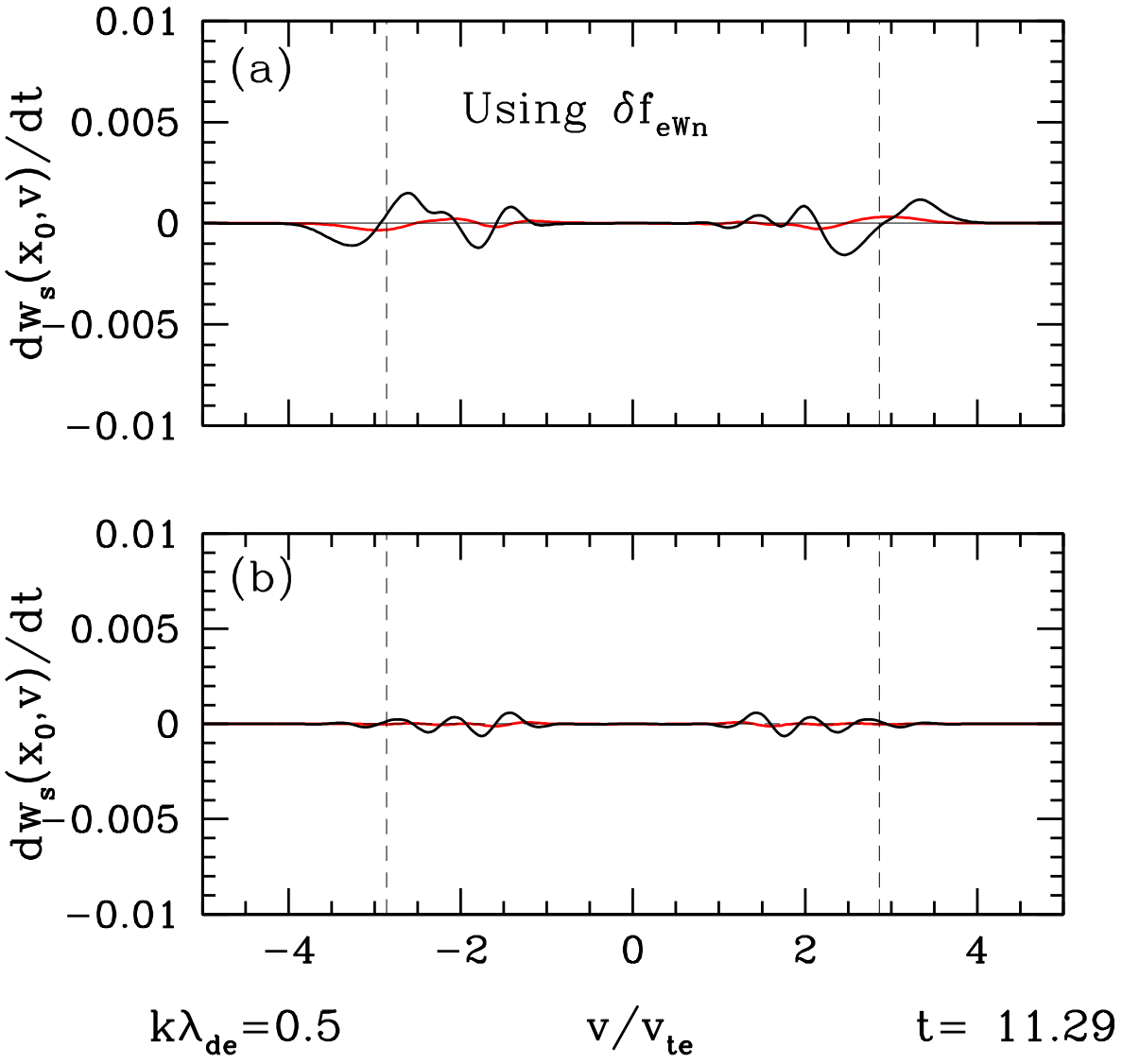

Figure 3.18: Plot of the (a) complete and (b) just even (in v) component of $q_e \frac{v^2}{2} \frac{\partial \delta f_{eWn}(x,v,t)}{\partial v} E(x_0,t)$ at $x_0 = 0$.

3.8 Notes

1. STARTEGY:Compare strongly and weakly damped runs, as well as linear and nonlinear runs to isolate the signal of Landau damping in the distribution function.

2. If we correlate separately the ballistic and wave perturbations with the fields, we should find that only the wave portion has a significant correlation. This means that, for the full distribution function, the correlation with the field should look very much like the correlation with just the wave portion! This is really helpful, as it demonstrates directly that you can sense just the important piece of the distribution function that corresponds to Landau damping (although it may be difficult to eliminate the wave portion of the energy transfer, because this will also show up). How can we differentiate the wave portion from the Landau damped portion?

3. Does some lag or phase shift indicate a secular energy transfer, as opposed to a simply oscillatory pattern?

4. Actually, the key is that the wave oscillation affects particles at all velocities equally (this is the fluid response), whereas the resonant wave-particle interaction affects only the particles near resonance!

5. GOAL OF PAPER on VP: Identify the energy transfer from waves to particles via Landau damping and isolate the perturbations to the distribution function associated with that transferred energy. Then, formulate a procedure (involving wave-particle corrlations) that can isolate just that secular energy transfer, even without the helpful decomposition of δf that we use to isolate the transferred energy. Show that this procedure produces similar (or exactly the same) results when applied to the unsplit δf in the VP code as proof that this works. Next paper will be to apply this procedure to GK simulations. Then to explore how this can be applied to single-point spacecraft measurements.

6. MAYBE write a PRL describing the basic technique and results, and a longer paper providing all the details—Kris would be PRL author, I would be longer JPP author. Tak Chu on papers as well. Since this is an important new technique, I think this is justified. Many of the basic statements in PRL about energy transfer and properties can be proven in detail in longer paper. (FIRST, just write longer paper and then separate out key results and figures for PRL!).

7. Publication strategy: Klein PRL on method using VP. Howes JPP with full details about VP case. Li PRL on application of method to AstroGK 3D OT simulations. Klein JPP on longer GK case—analytical with simplified GK results. NOTE: A simplified case with $\delta B_{\parallel} = 0$, to focus strictly on electron Landau damping, would be useful for Li PRL, because it would simplify things!

8. NOTE: Lots of energy transfer due to linear term (it is entirely odd), but this energy is strictly sinusoidal in space and therefore averages to zero. This is the oscillating wave energy. Probably with a sufficiently long averaged correlation, this goes away!

9. Note that in a linear run, the plasma never gains any energy since the ballistic term on ly moves energy and the linear wave-particle interaction term, although it leads to local energy changes, also does not lead to any net change in energy.

Bibliography